E-Publication: Online Open Access Vol: 68 Issue 10 | 2025

DOI: 10.5281/zenodo.17321958

PRECISION OXYGEN ACTIVATION BY NITRILE-SUBSTITUTED IRON-TPA COMPLEXES: FROM BIOMIMETIC OXIDATION TO POTENTIAL PRO-OXIDANT CANCER THERAPEUTICS

ZEINA S. MALEK

PhD, Physiology Professor, Faculty of Pharmacy, Arab International University, Damascus, Syria. Email: zeinasmalek@gmail.com, ORCID: 0009-0006-7075-7991

GHASSAN SHANNAN

B.Sc, PhD, Faculty of Pharmacy Dean, Arab International University, Damascus, Syria. Email: ghassan.shannan@outlook.com, ORCID: 0009-0005-9673-8564

Dr. NASSER THALLAJ*

Professor, Pharmaceutical Chemistry and Drug Quality Control Department, Faculty of Pharmacy, Arab International University, Damascus, Syria. *Corresponding Author Email: profthallaj@gmail.com, ORCID: 0000-0002-6279-768X, ¹Scopus ID: 59803999800, ²Scopus ID: 10044360600

Abstract

This study reports the synthesis and characterization of a series of nitrile-functionalized tris(2-pyridylmethyl) amine (TPA) ligands—CNTPA, (CN)₂TPA, and (CN)₃TPA—and their corresponding iron (II) complexes. Systematic introduction of nitrile groups at the α-position induces a pronounced electron-withdrawing effect, increasing the ligand oxidation potential by ~110 mV per nitrile substituent, as demonstrated by electrochemical analysis. These complexes react with molecular oxygen to form stable μ-oxo diferric species, which can be reversibly reduced to regenerate the ferrous precursors. Structural studies reveal distinct coordination geometries: while the parent TPA yields a symmetrical dicationic µ-oxo complex with κ⁴-N coordination, CNTPA forms a neutral symmetrical dimer, and (CN)₂TPA produces a neutral, asymmetrically bridged species. A key finding is the correlation between ligand-induced electron deficiency at the iron center and oxygenation kinetics, with increased Lewis's acidity accelerating O₂ activation. This supports a mechanism involving inner-sphere dioxygen coordination rather than outer-sphere electron transfer, which typically requires more negative reduction potentials. Furthermore, catalytic oxidation of cyclohexane to cyclohexanone under O₂, mediated by these complexes in the presence of zinc amalgam, demonstrates enhanced reactivity for (CN)₂TPAFeCl₂, aligning with its optimal balance of electronic activation and steric accessibility. These results highlight the critical role of ligand design in tuning metalcentered reactivity for small-molecule activation and catalytic oxidation processes.

Keywords: Iron (II) Complexes; Nitrile-Functionalized TPA Ligands; Electron-Withdrawing Effects; M-Oxo Diferric Species; Dioxygen Activation; Lewis's Acidity Modulation; Catalytic Cyclohexane Oxidation.

INTRODUCTION

The enzymatic transfer of oxygen to organic substrates represents a cornerstone of biological oxidation chemistry, with metalloproteins employing either heme-type iron centers (e.g., cytochromes P-450) or non-heme iron clusters (e.g., methane monooxygenase) to facilitate these transformations [1–6]. These systems harness molecular oxygen (O_2) as the primary oxidant, a process that necessitates its initial binding and subsequent activation. Mechanistically, O_2 activation can proceed via two

ISSN: 1673-064X

E-Publication: Online Open Access Vol: 68 Issue 10 | 2025

DOI: 10.5281/zenodo.17321958

dominant pathways: (i) formation of a metal-hydroperoxo intermediate (M-OOH) or (ii) homolytic or heterolytic O-O bond cleavage, yielding highly reactive metal-oxo species (M=O) [2-9]. The latter intermediates are particularly notable for their ability to mediate challenging C-H bond functionalization and oxygen insertion reactions under mild conditions. Inspired by these biological systems, synthetic chemists have developed ironbased coordination complexes to model and mimic enzymatic oxygen activation. Among these, iron (II) complexes supported by the tetradentate ligand tris(2-pyridylmethyl) amine (TPA) and its derivatives have emerged as prominent structural and functional analogues of non-heme iron oxygenases [3,7-18]. Despite significant progress, a persistent challenge in biomimetic chemistry is the preferential reliance on hydroperoxide oxidants (e.g., H₂O₂, ROOH) rather than direct O₂ activation [19–25]. While molecular oxygen can participate in these reactions, its reactivity in synthetic systems is typically restricted to ferrous (Fe2+) complexes pre-coordinated with strongly electron-donating substrates (e.g., catecholates, thiolates) that enhance metal-mediated O₂ binding [26–32]. Beyond hydrocarbon oxidation, oxygen-activating metalloenzymes play critical roles in neurotransmitter biosynthesis. A notable example is tryptophan hydroxylase, which catalyzes the rate-limiting step in serotonin production and influences circadian regulation [33–40]. The enzyme's dependence on iron and O₂ underscores the broader biological significance of controlled oxygen activation. In pursuit of synthetic systems capable of direct O₂ activation, our laboratory has investigated a series of dichloroferrous complexes supported by modified TPA-type ligands [41-49]. A key structural feature of these systems is the substitution pattern on the ligand's nitrogen donors, which modulates coordination geometry—shifting between tridentate and tetradentate binding modes. Intriguingly, halogen-substituted variants exhibit spontaneous reactivity with O₂ without requiring exogenous reductants or activating substrates. This behavior arises from a synergistic combination of steric constraints and electronic tuning, wherein electronwithdrawing substituents stabilize higher oxidation states while preventing deleterious ligand oxidation. A central objective in biomimetic oxidation catalysis is the rational design of artificial systems that replicate the efficiency and selectivity of metalloenzymes. Achieving this goal demands the integration of three critical components: (1) a redoxactive metal center capable of O₂ binding and activation, (2) a tunable electron reservoir (either intrinsic to the ligand or supplied externally), and (3) a protective microenvironment—modeled after protein matrices or engineered using inorganic (e.g., zeolites, electrodes) or organic (e.g., dendrimers, nanomaterials) scaffolds [50-58]. The development of such systems necessitates a library of well-characterized, functionally diverse complexes with predictable reactivity patterns. Within this framework, the present study focuses on the synthesis, characterization, and reactivity of TPA-derived ligands functionalized with nitrile groups (-CN) at one, two, or three pyridyl positions [59-67]. Nitrile substitution was selected for its ability to modulate both steric and electronic properties while maintaining ligand stability under oxidative conditions. [68-75] The corresponding dichloroferrous complexes were prepared and structurally characterized, with one derivative subjected to detailed solution-phase analysis. [76-78] Preliminary

ISSN: 1673-064X

E-Publication: Online Open Access Vol: 68 Issue 10 | 2025

DOI: 10.5281/zenodo.17321958

investigations into their reactivity with O_2 reveal distinct activation pathways, offering insights into the role of ligand architecture in governing oxygenase-like behavior [79–88]. This work advances the broader objective of developing functional synthetic analogues of non-heme iron oxygenases, with implications for catalytic C–H functionalization and sustainable oxidation chemistry. [89-96] By systematically varying ligand electronics and denticity, we aim to establish structure-reactivity correlations that inform the design of next-generation oxidation catalysts. [97-104]

The nitrile-functionalized iron-TPA complexes developed in this study offer a novel catalytic approach to cancer therapy by exploiting tumor-specific oxidative vulnerabilities. [105-112] These complexes can selectively generate reactive oxygen species (ROS) within cancer cells through controlled O_2 activation, mimicking enzymatic processes but with tunable reactivity. Key therapeutic mechanisms include:

- **1. Targeted Oxidative Stress** The complexes catalyze sustained ROS production, overwhelming cancer cells that already operate under elevated oxidative stress, while sparing normal cells with robust antioxidant defenses [113-120].
- **2. Hypoxia Compatibility** Unlike radiation or conventional drugs, these O₂-activating complexes remain functional in hypoxic tumor microenvironments where traditional therapies fail [121-128].
- 3. Redox Cycling Zinc-mediated reduction allows catalytic regeneration of active Fe (II) species, enabling prolonged ROS generation at low doses. [129-136]
- **4. Selective DNA/Lipid Damage** High-valent iron-oxo intermediates can oxidize DNA bases and membrane lipids, inducing lethal cellular damage. [137-146]

By optimizing ligand electronics, these complexes may be tailored for specific cancers, offering a new class of pro-oxidant therapeutics that operate through fundamentally distinct, biomimetic mechanisms. [147-150]

Experimental Section: Synthesis and Characterization of Nitrile-Functionalized TPA Ligands

1. Synthesis of 2-Cyano-6-methylpyridine

A solution of 2-methylpyridine-1-oxide (24.6 g, 0.200 mol) in anhydrous dichloromethane (200 mL) was dried over magnesium sulfate and transferred via cannula to a reaction flask containing trimethylsilyl cyanide (25.0 g, 0.253 mol). A solution of dimethylcarbamyl chloride (21.4 g, 0.253 mol) in dichloromethane (50 mL) was added dropwise over 30 min. The reaction mixture was stirred for 24 h at ambient temperature, after which a 10% aqueous potassium carbonate solution (200 mL) was added slowly. The organic product was extracted with dichloromethane (3 \times 50 mL), and the combined organic phases were dried over MgSO₄. Solvent removal under reduced pressure followed by recrystallization from pentane afforded 2-cyano-6-methylpyridine as a white crystalline solid (26.0 g, 0.220 mol, 98% yield).

ISSN: 1673-064X

E-Publication: Online Open Access

Vol: 68 Issue 10 | 2025 DOI: 10.5281/zenodo.17321958

1H NMR (CDCI₃, 400 MHz): δ 7.70 (t, 1H, CHγ), 7.50 (d, 1H, CHβ'), 7.37 (d, 1H, CHβ), 2.60 (s, 3H, CH₃).

2. Synthesis of 2-Cyano-6-(bromomethyl)pyridine

A mixture of 2-cyano-6-methylpyridine (10.0 g, 0.084 mol), N-bromosuccinimide (16.6 g, 0.093 mol), and benzoyl peroxide (0.2 g, 0.840 mmol) in carbon tetrachloride (200 mL) was refluxed (90 °C) for 6 h under vigorous stirring. After cooling, the precipitated succinimide was removed by filtration, and the solvent was evaporated under reduced pressure. The crude product was purified by silica gel column chromatography (toluene eluent), yielding 2-cyano-6-(bromomethyl) pyridine as a pale-yellow solid (3.0 g, 0.015 mol, 18% yield).

1H NMR (CDCI₃, 400 MHz): δ 7.86 (t, 1H, CH γ), 7.69 (dd, 1H, CH β '), 7.62 (dd, 1H, CH β), 4.55 (s, 2H, CH $_2$ Br).

3. Synthesis of TPACN (Tris(2-cyano-6-pyridylmethyl) amine)

A solution of 2-cyano-6-(bromomethyl) pyridine (1.00 g, 5.07 mmol), dimethylpyridineamine (1.01 g, 5.07 mmol), and sodium carbonate (0.54 g, 5.07 mmol) in acetonitrile (100 mL) was refluxed (95 °C) for 18 h. The reaction mixture was filtered to remove inorganic salts, and the solvent was evaporated. The residue was extracted with dichloromethane/water, dried (MgSO₄), and recrystallized from pentane to afford TPACN as a white solid (1.29 g, 4.11 mmol, 81% yield).

Elemental Analysis: Found: C, 72.63%; H, 5.08%; N, 22.42%. Calc. for $C_{24}H_{18}N_6$: C, 72.36%; H, 5.43%; N, 22.21%.

1H NMR (CDCI₃, 400 MHz): δ 8.53 (m, 2H, CHα), 7.82 (dd, 1H, CHβ1), 7.77 (t, 1H, CHγ1), 7.65 (td, 2H, CHγ), 7.54 (dd, 1H, CHβ1'), 7.51 (dt, 2H, CHβ'), 7.15 (m, 2H, CHβ), 3.92 (s, 2H, CH₂), 3.88 (s, 4H, CH₂).

13C NMR (CDCI₃, 100 MHz): δ 162 (2'), 159 (2), 149 (6), 137 (4'), 136 (4), 132 (6'), 127 (3'), 126 (5'), 123 (3), 122 (5), 117 (CN), 60 (CH₂), 59 (CH₂).

IR (KBr): $v(CN) = 2539 \text{ cm}^{-1}$.

4. Synthesis of TPACN₂ (Bis(2-cyano-6-pyridylmethyl) (2-pyridylmethyl) amine)

A mixture of 2-cyano-6-(bromomethyl) pyridine (1.40 g, 7.10 mmol), picolylamine (0.40 g, 3.55 mmol), and sodium carbonate (0.37 g, 3.55 mmol) in acetonitrile (100 mL) was refluxed (95 °C) for 18 h. Workup as described for TPACN afforded TPACN $_2$ as a white solid (1.17 g, 3.44 mmol, 97% yield).

Elemental Analysis: Found: C, 70.18%; H, 4.79%; N, 24.23%. Calc. for $C_{20}H_{15}N_5$: C, 70.57%; H, 4.74%; N, 24.69%.

1H NMR (CDCI₃, 400 MHz): δ 8.545 (m, 1H, CH α), 7.802 (dd, 2H, CH β 1), 7.794 (dd, 2H, CH β 1'), 7.665 (td, 1H, CH γ), 7.566 (dd, 2H, CH γ 1), 7.473 (dt, 1H, CH β 1'), 7.169 (m, 1H, CH β 1), 3.993 (s, 4H, CH γ 2), 3.889 (s, 2H, CH γ 2).

ISSN: 1673-064X

E-Publication: Online Open Access

Vol: 68 Issue 10 | 2025 DOI: 10.5281/zenodo.17321958

13C NMR (CDCI₃, 100 MHz): δ 161 (2'), 158 (2), 149 (6), 137 (4'), 136 (4), 133 (6'), 127 (3'), 126 (5'), 123 (3), 122 (5), 117 (CN), 60 (CH₂), 59 (CH₂).

IR (KBr): $v(CN) = 2536 \text{ cm}^{-1}$.

5. Synthesis of TPACN₃ (Tris(2-cyano-6-pyridylmethyl) amine)

A sealed flask containing 2-cyano-6-(bromomethyl) pyridine (3.00 g, 15.23 mmol), ammonium chloride (0.26 g, 4.08 mmol), and sodium hydroxide (0.20 g, 5.08 mmol) in THF

(100 mL) was stirred for 72 h. After filtration and solvent removal, the crude product was purified by silica gel chromatography (gradient elution: $CH_2Cl_2 \rightarrow CH_2Cl_2$ /acetone 1:1) to afford TPACN₃ as a white solid (4.1 g, 11.23 mmol, 74% yield).

Elemental Analysis: Found: C, 69.33%; H, 4.30%; N, 26.47%. Calc. for $C_{24}H_{18}N_6$: C, 69.04%; H, 4.11%; N, 26.85%.

1H NMR (DMSO-d₆, 400 MHz): δ 7.99 (t, 3H, CHγ1), 7.88 (d, 3H, CHβ1'), 7.85 (d, 3H, CHβ1), 3.94 (s, 6H, CH₂).

13C NMR (DMSO-d₆, 100 MHz): δ 161 (2), 139 (4), 132 (6), 128 (3), 127 (5), 118 (CN), 60 (CH₂).

IR (KBr): $v(CN) = 2538 \text{ cm}^{-1}$.

DISCUSSION OF SYNTHETIC METHODOLOGY

The stepwise functionalization of the TPA scaffold with nitrile groups was achieved via nucleophilic substitution, with yields ranging from 18% (bromination) to 97% (TPACN₂). The nitrile stretches (v(CN) \approx 2536–2539 cm⁻¹) in the IR spectra confirmed successful incorporation of the cyano moiety. NMR and elemental analysis validated the structural integrity of all derivatives, setting the stage for subsequent coordination studies with iron (II).

RESULTS AND DISCUSSION

Strategic Approach to Ligand Design and Synthesis

The present work focuses on the systematic development of α -substituted TPA (tris(2-pyridylmethyl) amine) derivatives, specifically targeting mono-, di-, and tri- functionalized variants. While the preparation of α -substituted pyridine precursors is typically straightforward, the synthesis of 2-cyano-6-methylpyridine presented particular challenges due to its pronounced sensitivity to trace moisture. Optimal purification was achieved through recrystallization from pentane or hexane, yielding the desired product as a pale yellow crystalline solid.

The synthetic strategy employed nucleophilic aromatic substitution chemistry, utilizing non-commercial halomethylpyridine intermediates that required custom synthesis

E-Publication: Online Open Access

Vol: 68 Issue 10 | 2025 DOI: 10.5281/zenodo.17321958

(Figure 1). This approach proved particularly effective for constructing the target ligand architectures through controlled functionalization of the TPA core structure.

Figure 1: preparation of the starting materials necessary these products are not commercialy availale.

Ligand Synthesis and Characterization

Three distinct nitrile-functionalized TPA derivatives were successfully prepared and characterized:

1. CNTPA Synthesis:

The mono-substituted derivative was obtained via a classical SN2 reaction between bis(2-pyridylmethyl) amine (DPA) and 6-cyano-2-(bromomethyl)pyridine in the presence of base. This transformation proceeded efficiently when employing a slight excess of DPA (readily removable by distillation), typically yielding the desired product in approximately 90% yield.

2. (CN)₂TPA Synthesis:

The disubstituted analogue was prepared through stoichiometric reaction of picolylamine with two equivalents of 6-cyano-2-(bromomethyl)pyridine under basic conditions. This approach allowed for controlled bis-functionalization while maintaining excellent reaction selectivity.

E-Publication: Online Open Access

Vol: 68 Issue 10 | 2025 DOI: 10.5281/zenodo.17321958

3. (CN)₃TPA Synthesis:

The trisubstituted variant was synthesized through an in-situ ammonia generation protocol, where sodium hydroxide-mediated decomposition of ammonium chloride produced the required nucleophile in a sealed reaction vessel.

The resulting product exhibited limited solubility in common organic solvents, a characteristic that facilitated its purification by selective precipitation.

All synthesized ligands were obtained as white crystalline solids following recrystallization from pentane (Figure 2). Comprehensive characterization was performed using elemental analysis, multinuclear NMR spectroscopy (¹H and ¹³C), infrared spectroscopy, and cyclic voltammetry, confirming both the structural integrity and purity of each compound.

Figure 2: Preparation of (TPA) series respectively CNTPA, (CN)2TPA and (CN)3TPA.

The infrared spectra of all derivatives exhibited characteristic nitrile stretching vibrations (v(C≡N)) in the 2250-2300 cm⁻¹ range, while NMR analysis revealed the expected

Yield 74%

E-Publication: Online Open Access

Vol: 68 Issue 10 | 2025 DOI: 10.5281/zenodo.17321958

patterns for the asymmetrically substituted pyridine rings. Electrochemical studies demonstrated the influence of progressive nitrile substitution on the redox properties of the TPA framework, providing valuable insights for subsequent coordination chemistry investigations.

This systematic synthetic approach has successfully generated a series of tunable TPAtype ligands with varying degrees of nitrile functionalization, establishing a robust platform for the development of novel iron coordination complexes with tailored electronic and steric properties.

Comparative Electrochemical Analysis of Nitrile-Functionalized TPA Ligands

The electrochemical properties of the synthesized CNTPA, (CN)₂TPA, and (CN)₃TPA ligands were systematically investigated using cyclic voltammetry in anhydrous acetonitrile at ambient temperature (298 K). All measurements were conducted under inert atmosphere conditions employing a standard three-electrode configuration (platinum working and counter electrodes, saturated calomel reference electrode [SCE]), with 0.1 M tetrabutylammonium hexafluorophosphate (TBAPF₆) as supporting electrolyte. Scan rates were maintained at 200 mV/s to ensure optimal resolution of redox events while minimizing capacitive current contributions. For comparative analysis, the voltammetric behavior of the parent TPA ligand was included as a benchmark (Figure 3).

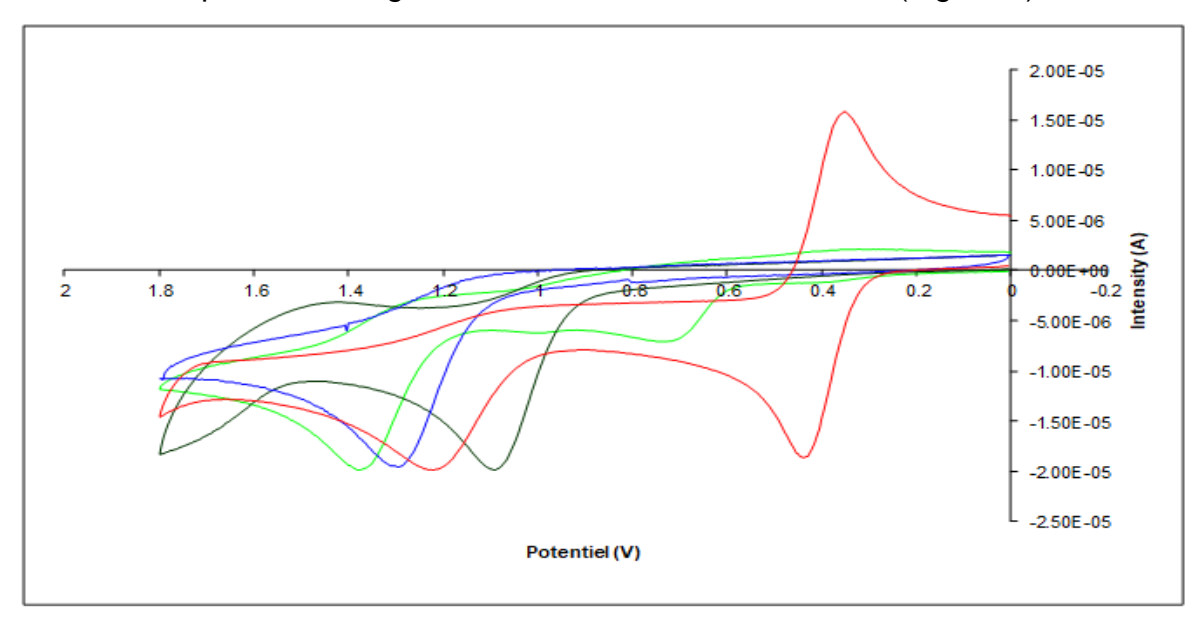


Figure3: Voltammerogram of ligands (TPA; CNTPA; (CN)2TPA; and (CN)3TPA), with TPA in black, CNTPA in red, (CN)2 TPAin blue, (CN)3TPAin green.

	TPA	CNTPA	(CN)2TPA	(CN)3TPA
E _a (V/ECS)	1.12	1.25	1.34	1.45

The cyclic voltammograms revealed distinct oxidation events for each ligand, all exhibiting irreversible anodic waves corresponding to single-electron oxidation of the tertiary amine

ISSN: 1673-064X

E-Publication: Online Open Access Vol: 68 Issue 10 | 2025

DOI: 10.5281/zenodo.17321958

center. The oxidation potentials (E_a) demonstrated a progressive positive shift with increasing nitrile substitution: TPA (1.12 V), CNTPA (1.25 V), (CN)₂TPA (1.34 V), and (CN)₃TPA (1.45 V) versus SCE. This systematic variation reflects a consistent potential increase of approximately 110 mV per additional nitrile group, mirroring trends previously observed in fluorinated TPA analogues. Notably, the (CN)₃TPA voltammogram displayed an additional low-intensity irreversible oxidation at 0.73 V/SCE, the origin of which remains unclear but may suggest either:

- 1. Partial decomposition products from ligand synthesis.
- 2. Oxidation of trace impurities in the sample.

The reversible redox couple observed at $E_1/_2 = 0.382$ V/SCE was assigned to the ferrocene/ferrocenium internal reference. The marked positive potential shifts observed with increasing nitrile substitution quantitatively demonstrate the strong electron-withdrawing character of the cyano groups, which effectively stabilize the highest occupied molecular orbital (HOMO) of the ligand framework. This electronic perturbation has significant implications for the redox properties of resulting metal complexes, particularly in modulating metal-centered oxidation states during catalytic cycles.

These electrochemical findings provide crucial insights into the electronic structure modifications imparted by progressive nitrile functionalization, establishing a clear structure- property relationship that informs the design of tunable ligand platforms for oxidation catalysis. The consistent potential shifts confirm the additive nature of electronic effects in this ligand series, offering predictable control over the redox properties of derived coordination complexes.

Synthesis and Characterization of Iron (II) Complexes with Nitrile-Functionalized TPA Ligands

All metal coordination reactions were conducted under rigorously controlled anaerobic conditions employing standard Schlenk line techniques and an argon atmosphere. Solvent preparation involved meticulous purification through fractional distillation followed by three successive freeze-pump-thaw cycles to ensure complete oxygen removal. The synthetic methodology comprised the sequential cannula transfer of anhydrous tetrahydrofuran (100 mL) to a Schlenk flask containing anhydrous ferrous chloride (0.9 equivalents), followed by transfer to a second Schlenk vessel containing the respective TPA-based ligand (CNTPA, (CN)₂TPA, or (CN)₃TPA; 0.2 g, 1 equivalent). A 10% molar excess of ligand was employed to compensate for potential processing losses while maintaining reaction stoichiometry.

Immediate colorimetric changes to characteristic reddish solutions upon mixing provided visual confirmation of complex formation. The reaction mixtures were stirred continuously for 10 hours at 298 K to ensure complete coordination. Workup procedures involved cannula filtration under inert atmosphere, followed by solvent evaporation under reduced pressure. Subsequent purification was achieved through dissolution in anhydrous

E-Publication: Online Open Access

Vol: 68 Issue 10 | 2025

DOI: 10.5281/zenodo.17321958

acetonitrile and precipitation with diethyl ether, with thorough ether washing to remove residual reactants. Final products were isolated as microcrystalline solids following overnight vacuum desiccation.

$$L + FeCl_2 \xrightarrow{THF \text{ ou } CH_3CN} LFeCl_2$$

$$R_1 = R_1 = CN, R_2 = R_3 = H$$

$$(CN)_2TPA: R_1 = R_2 = CN, R_3 = H$$

$$(CN)_3TPA: R_1 = R_2 = R_3 = CN$$

Physicochemical Characterization

The synthesized iron (II) complexes were comprehensively characterized using an array of spectroscopic and analytical techniques:

- **1. UV-Vis Spectrophotometry**: Revealed ligand-to-metal charge transfer (LMCT) bands and d-d transitions diagnostic of the coordination environment.
- **2. Paramagnetic** ¹H NMR Spectroscopy: Provided structural insights despite expected line broadening effects characteristic of high-spin iron (II) systems.
- **3. Electrochemical Analysis**: Cyclic voltammetry experiments elucidated the redox behavior and electronic effects imparted by nitrile substitution.
- **4. Conductivity Measurements**: Assessed the ionic character and potential electrolyte behavior in solution.
- **5. Single-Crystal X-ray Diffraction**: Where feasible, provided definitive structural determination of molecular geometry and bonding parameters.

While the coordination reactions are presumed quantitative based on stoichiometric considerations, minor product losses were encountered during purification steps, particularly during solvent transfer and precipitation stages. The consistent reddish coloration observed across all complexes suggests analogous coordination geometries, though subtle variations in spectral features reflect the electronic perturbations induced by progressive nitrile substitution. This comprehensive characterization approach

E-Publication: Online Open Access Vol: 68 Issue 10 | 2025

DOI: 10.5281/zenodo.17321958

enables rigorous correlation between ligand architecture and complex properties, particularly regarding electronic.

I. Spectroscopic Characterization of Iron (II) Complexes by UV-Visible Spectroscopy

The electronic absorption spectra of the synthesized iron (II) complexes (CNTPAFeIICl₂, (CN)₂TPAFeIICl₂, and (CN)₃TPAFeIICl₂) exhibit two distinct absorption features as shown in Figure 4. The higher-energy transitions observed between 258-269 nm (ϵ = 9743-12046 M⁻¹cm⁻¹) are characteristic of $\pi \rightarrow \pi^*$ electronic excitations within the pyridyl rings of the TPA ligand framework [66-73].

More significantly, broad metal-to-ligand charge transfer (MLCT) bands appear at longer wavelengths (389-471 nm, ϵ = 759-1963 M⁻¹cm⁻¹), as summarized in Table 1. These MLCT transitions demonstrate substantial bathochromic shifts and tailing into the visible region, accounting for the intense coloration of the complexes. Specifically, the (CN)₂TPAFeIICl₂ (λ max = 471 nm) and (CN)₃TPAFeIICl₂ (λ max = 451 nm) complexes exhibit absorption maxima in the blue-green region, resulting in their observed reddish hues. In contrast, CNTPAFeIICl₂ (λ max = 389 nm) displays a red-orange coloration due to its predominant absorption in the blue-violet spectral region.

The systematic variation in both absorption maxima and molar extinction coefficients (ϵ) with increasing nitrile substitution reveals important electronic perturbations within the coordination sphere. The progressive red-shift of the MLCT bands and decreasing extinction coefficients from CNTPA to (CN) $_3$ TPA derivatives suggest enhanced delocalization of electron density from the iron center to the π -accepting nitrile-modified ligands. These spectroscopic observations provide direct evidence for the significant electronic effects imparted by progressive nitrile functionalization on the frontier molecular orbitals of the complexes.

Table 1: UV-visible data of the CNTPAFeCl₂, (CN)2TPAFeCl₂ and (CN)3TPAFeCl₂ complexes and their molar extinction coefficients.

CNTPAFe ^{II} CI₂	(CN)₂TPAFe ^{II} CI₂	(CN)₃TPAFe ^{II} CI₂
λ, nm, (ε, mmole ⁻¹ .cm ⁻²)	λ, nm, (ε, mmole ⁻¹ .cm ⁻²)	λ, nm, (ε, mmole ⁻¹ .cm ⁻²)
258 (9743)	262 (10811)	269 (12046)
389 (1963)	471 (1127)	451 (759)

More significantly, broad metal-to-ligand charge transfer (MLCT) bands appear at longer wavelengths (389-471 nm, ϵ = 759-1963 M⁻¹cm⁻¹), as summarized in Table 1. These MLCT transitions demonstrate substantial bathochromic shifts and tailing into the visible region, accounting for the intense coloration of the complexes. Specifically, the (CN)₂TPAFeIICl₂ (λ max = 471 nm) and (CN)₃TPAFeIICl₂ (λ max = 451 nm) complexes exhibit absorption maxima in the blue-green region, resulting in their observed reddish hues. In contrast, CNTPAFeIICl₂ (λ max = 389 nm) displays a red-orange coloration due to its predominant absorption in the blue-violet spectral region.

E-Publication: Online Open Access Vol: 68 Issue 10 | 2025

DOI: 10.5281/zenodo.17321958

The systematic variation in both absorption maxima and molar extinction coefficients (ϵ) with increasing nitrile substitution reveals important electronic perturbations within the coordination sphere. The progressive red-shift of the MLCT bands and decreasing extinction coefficients from CNTPA to (CN) $_3$ TPA derivatives suggest enhanced delocalization of electron density from the iron center to the π -accepting nitrile-modified ligands. These spectroscopic observations provide direct evidence for the significant electronic effects imparted by progressive nitrile functionalization on the frontier molecular orbitals of the complexes.

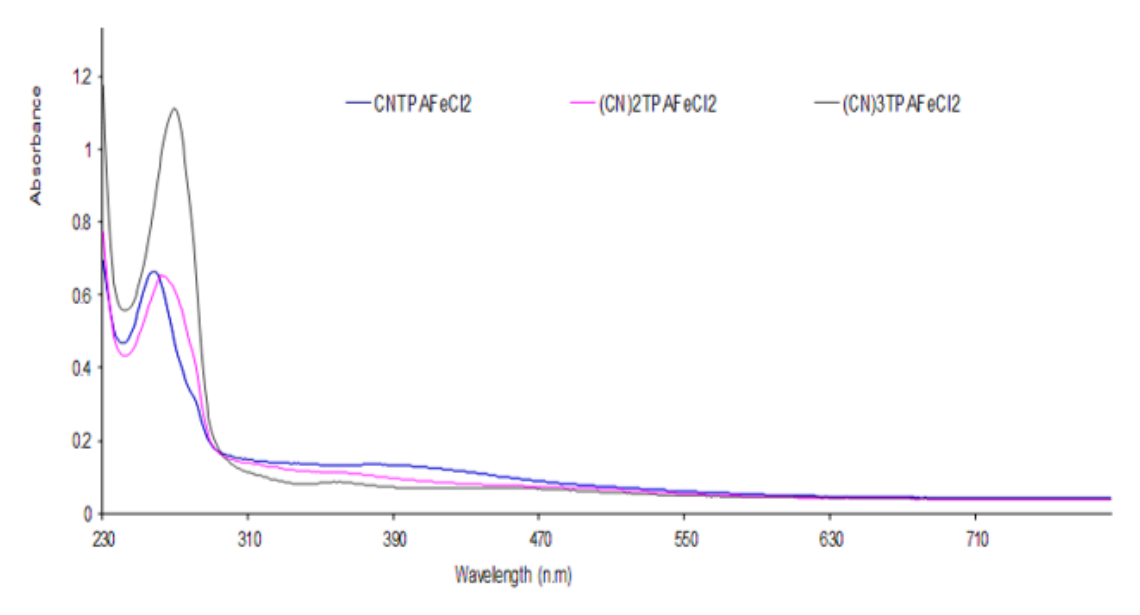


Figure 4: UV-visible spectra of the CNTPAFeCl2, (CN)2TPAFeCl2, and (CN)3TPAFeCl2 complexes.

II. Paramagnetic ¹H NMR Spectroscopic Analysis in CD₃CN

While less commonly employed in molecular characterization, paramagnetic ¹H NMR spectroscopy proves particularly informative for investigating electronic structure in paramagnetic complexes such as our iron (II) derivatives. The high-spin Fe²⁺ center (3d⁶ configuration, S = 2) induces substantial paramagnetic shifts (-50 < δ < 200 ppm) and significant line broadening, as evidenced in Figure 5. The observed resonance patterns confirm the strong spin-coupled nature of these complexes through their characteristic paramagnetic dispersion.

The proton resonances separate into two distinct categories based on their proximity to the paramagnetic center:

- 1. **Highly broadened signals** (α-pyridyl and CH₂ protons) demonstrating extensive hyperfine coupling due to their immediate coordination sphere environment
- 2. **Relatively sharper resonances** (β , β ', and γ protons) exhibiting reduced paramagnetic effects with increasing distance from the metal center.

E-Publication: Online Open Access

Vol: 68 Issue 10 | 2025 DOI: 10.5281/zenodo.17321958

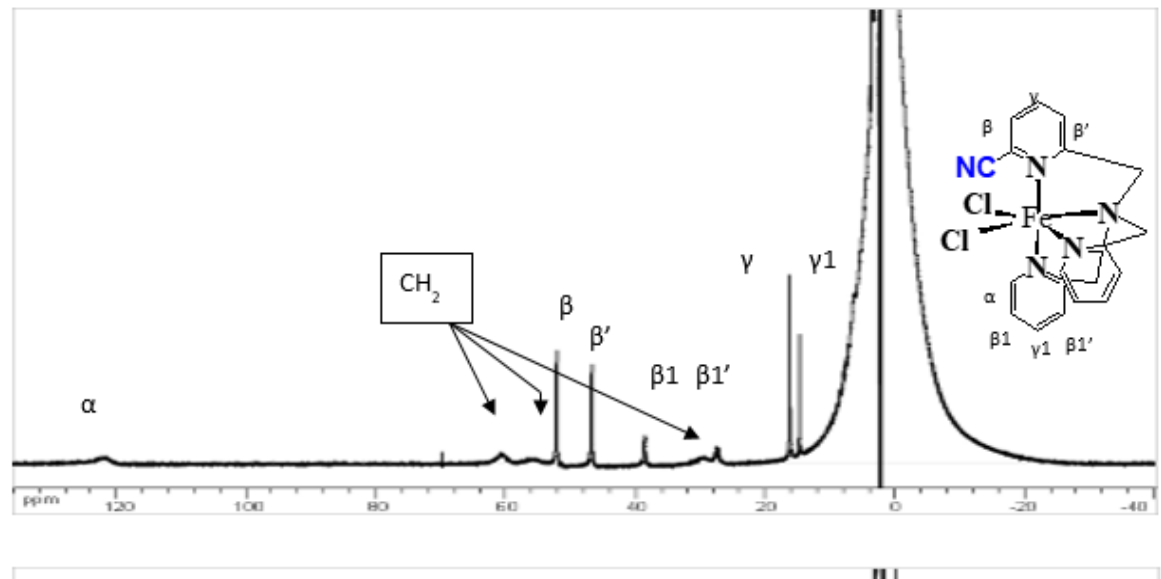
Linewidth analysis ($\Delta v_1/_2$) reveals a progressive broadening trend:

CNTPAFeCl₂: 50-51 Hz

(CN)₂TPAFeCl₂: 102-138 Hz

• (CN)₃TPAFeCl₂: >170 Hz

The well-resolved spectra obtained for mono- and di-substituted complexes (Figure 5) permitted complete assignment through comparative analysis with known structural analogues, particularly BrTPAFeCl₂ [2,13,23-27,60-73]. The observed paramagnetic shifts and linewidths for CNTPAFeCl₂ closely resemble those of BrTPAFeCl₂, consistent with a pseudo-octahedral coordination geometry



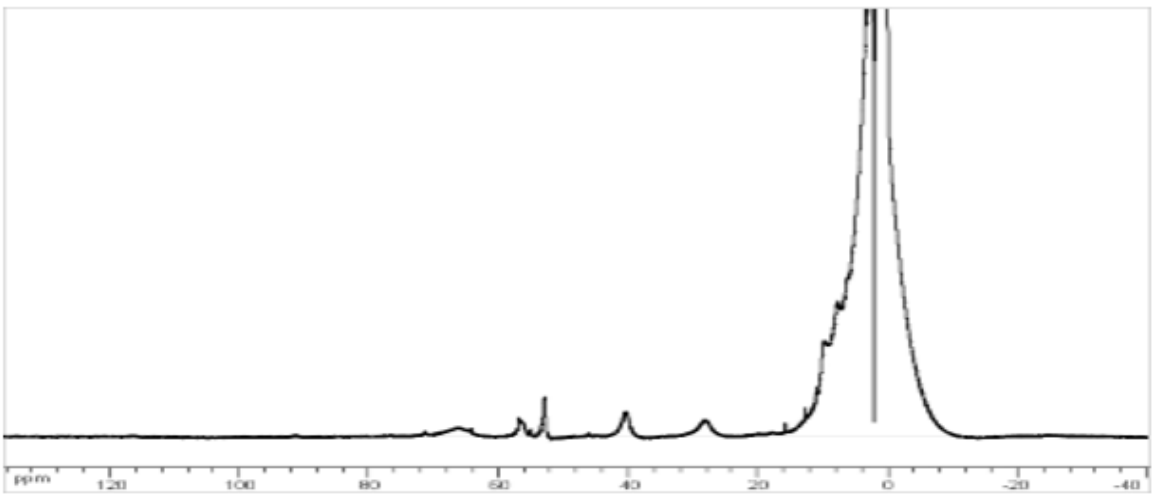


Figure 5: Paramagnetic 1H NMR spectrum for the CNTPAFeCl2 and (CN) 2TPAFeCl2 complexes.

E-Publication: Online Open Access

Vol: 68 Issue 10 | 2025 DOI: 10.5281/zenodo.17321958

The well-resolved spectra obtained for mono- and di-substituted complexes (Figure 5) permitted complete assignment through comparative analysis with known structural analogues, particularly BrTPAFeCl₂ [2,13,23-27,60-73]. The observed paramagnetic shifts and linewidths for CNTPAFeCl₂ closely resemble those of BrTPAFeCl₂, consistent with a pseudo-octahedral coordination geometry.

Notably, (CN)₃TPAFeCl₂ exhibits anomalous behavior (Figure 6). The unexpectedly narrow resonances juxtaposed with broad features contradict predictions based on its UV-visible characteristics (notably reduced MLCT extinction coefficient), which would suggest a trigonal bipyramidal geometry analogous to Br₃TPAFeCl₂ [13,23-27,60-73].

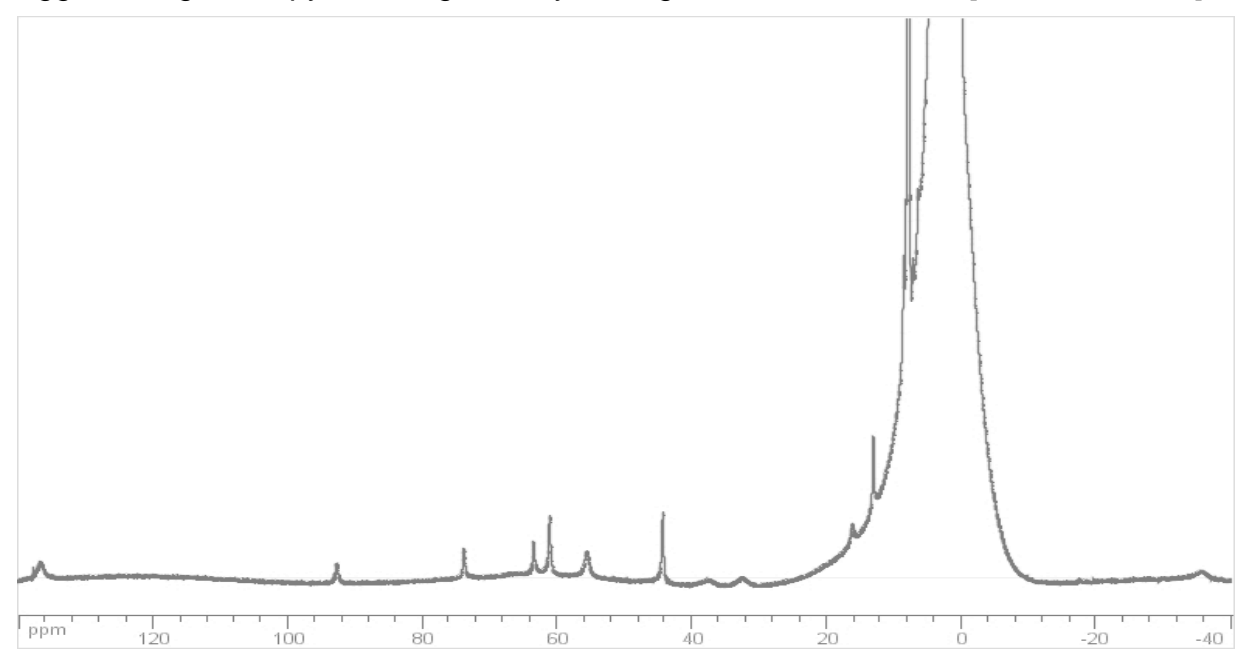


Figure 6: Paramagnetic 1H NMR spectrum obtained after dissolution in CD3CN of the (CN)3TPAFeCl2 complex

This spectroscopic discrepancy persists under rigorously anaerobic conditions, suggesting potential solvent-mediated effects. The presence of residual water (including D_2O) in deuterated acetonitrile may promote ligand exchange or hydrolysis, as will be discussed in subsequent sections [54-59]. These observations underscore the importance of complementary characterization techniques when investigating paramagnetic systems in protic media.

III. Conductometric Analysis of Iron (II) Complexes

Solution-phase conductivity measurements were conducted in anhydrous acetonitrile at 298 K to elucidate the ionic character of the synthesized complexes. The molar conductivities (Λ) were determined at standardized concentrations of approximately 1.0 \times 10⁻³ M, with the resulting values presented in Table 2.

ISSN: 1673-064X

E-Publication: Online Open Access Vol: 68 Issue 10 | 2025

DOI: 10.5281/zenodo.17321958

The observed conductivity values fall within a relatively narrow range:

• TPAFeCl₂: 30.34 S·mol⁻¹·cm²

• CNTPAFeCl₂: 13.80 S·mol⁻¹·cm²

(CN)₂TPAFeCl₂: 21.03 S⋅mol⁻¹⋅cm²

(CN)₃TPAFeCl₂: 25.15 S·mol⁻¹·cm²

These conductivity measurements provide critical insight into the solution behavior of the complexes. The measured Λ values are substantially lower than the characteristic range for singly-charged (1:1) electrolyte species in acetonitrile (typically ≥100 S·mol⁻¹·cm²) [60-73]. This significant discrepancy strongly suggests that all complexes maintain their neutral character in solution, existing predominantly as [Fe (TPA-R) Cl₂] species rather than dissociated ionic forms.

Table 2: Molar conductimetry measurements show that the complexes in solution remain neutral

	TPAFeCl ₂	CNTPAFeCl ₂	(CN) ₂ TPAFeCl ₂	(CN) ₃ TPAFeCl ₂
Λ(S.mol ⁻¹ .cm ²)	30.34	13.80	21.03	25.15

The observed trend in conductivity values among the series may reflect subtle variations in:

- 1. Molecular dipole moments induced by asymmetric nitrile substitution
- 2. Solvent-solute interactions modulated by ligand polarity
- 3. Minor differences in ion-pair dissociation equilibria

These findings are consistent with previous conductometric studies of analogous dichloroferrous complexes, further supporting the conclusion of neutral complex persistence in acetonitrile solution. The relatively low conductivity values effectively rule out significant formation of charged species under these experimental conditions, confirming the integrity of the neutral coordination spheres in solution.

Structural Characterization by Single-Crystal X-ray Diffraction

Single crystals suitable for X-ray diffraction analysis were obtained through vapor diffusion of diisopropyl ether into oxygen-free acetonitrile solutions of the complexes, prepared and sealed under inert atmosphere in glass tubes. Successful crystal growth was achieved for both CNTPAFeCl₂ and (CN)₂TPAFeCl₂ complexes using this methodology.

Crystal Structure of CNTPAFeCl₂

The complex crystallizes in the monoclinic space group P2₁/n with unit cell parameters a = 8.5600(5) Å, b = 15.5940(9) Å, c = 14.7230(11) Å, and β = 103.271(2) ° (α = γ = 90°), containing Z = 4 formula units per unit cell. Figure 7 presents the Mercury visualization of the molecular structure, with key metrical parameters provided in Table 3.

E-Publication: Online Open Access

Vol: 68 Issue 10 | 2025 DOI: 10.5281/zenodo.17321958

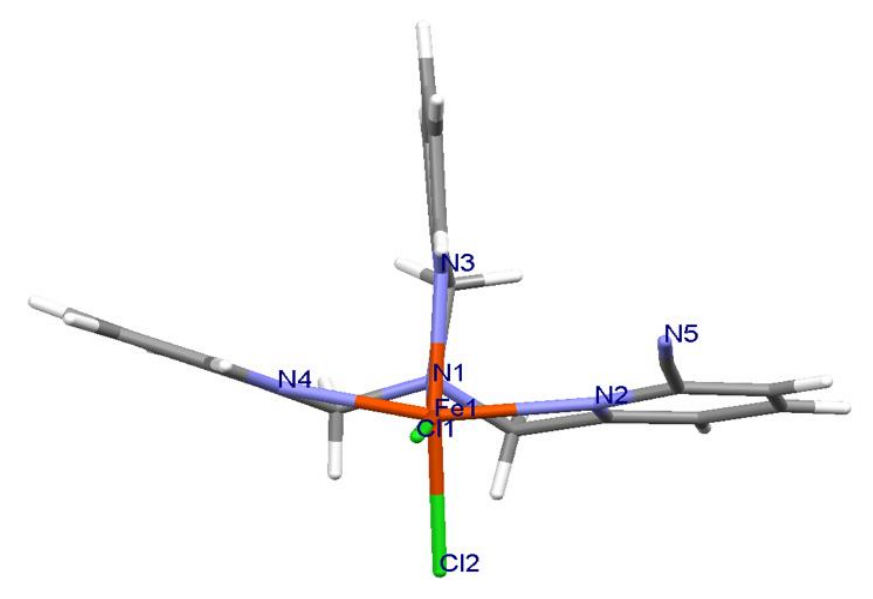


Figure 7: Mercury representation of the CNTPAFeCl₂ complex. The main distances and angles are given inTable 3.

Crystal Structure of (CN)₂TPAFeCl₂

This derivative likewise crystallizes in the monoclinic P2₁/n space group with unit cell dimensions a = 12.465(4) Å, b = 14.212(5) Å, c = 13.312(5) Å, and β = 102° (α = γ = 90°), with Z = 4. The molecular structure is depicted in Figure 8, with relevant bond metrics compiled in Table 3.

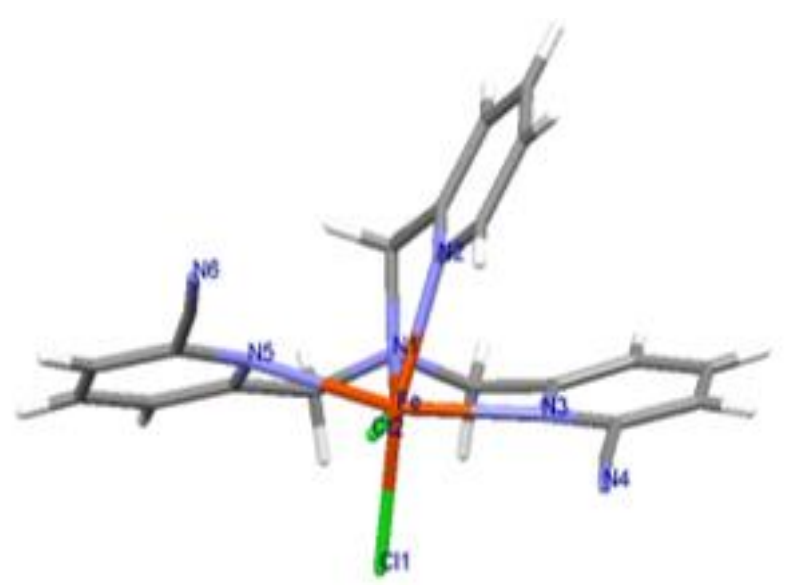


Figure 8: Mercury representation of the (CN)2TPAFeCl₂ complex. The main distances and angles are given in Table 3.

E-Publication: Online Open Access Vol: 68 Issue 10 | 2025

DOI: 10.5281/zenodo.17321958

Table 3: Interatomic distances and principal angles in CNTPAFeCl₂, (CN)₂TPAFeCl₂ complexes.

(CN) ₂ TPAFeCl ₂		CNTPAFeC1 ₂	
Les distances	Les angles	Les distances	Les angles
Fe N2 2.189(3)Å	N2 Fe N1 77.59(9)° N2 Fe Cl2 95.33(7)°	Fe1 N3 2.202(4)Å	N3 Fe1 N1 81.26(15)° N3 Fe1 N2 77.34(16)°
Fe N1 2.234(2)Å	N1 Fe Cl2 165.28(7)° N2 Fe N3 77.95(10)°	Fe1 N1 2.215(4)Å	N1 Fe1 N2 75.53(16)° N3 Fe1 N4 83.02(15)°
Fe C12 2.3217(8)Å	N1 Fe N3 76.21(9)° C12 Fe N3 115.30(7)° N2 Fe C11 163.76(7)°	Fe1 N2 2.266(4)Å	N1 Fe1 N4 146.20(17)° N2 Fe1 N4 71.92(16)°
Fe N3 2.325(3)Å	N1 Fe Cl1 90.89(7)° Cl2 Fe Cl1 98.35(3)°	Fe1 N4 2.312(4)Å	N3 Fe1 Cl1 97.20(12)° N1 Fe1 Cl1 96.98(13)° N2 Fe1 Cl1 171.22(12)°
Fe Cl1 2.3976(10)Å	N3 Fe C11 88.28(7)° N2 Fe N5 92.14(10)°	Fe1 C11 2.3496(15)Å	N4 Fe1 Cl1 171.22(12) N4 Fe1 Cl1 114.58(12)° N3 Fe1 Cl2 166.97(12)°
Fe N5 2.414(3)Å	N1 Fe N5 70.39(9)° Cl2 Fe N5 97.30(6)° N3 Fe N5 146.49(9)° Cl1 Fe N5 94.75(7)° C12 N3 Fe 129.3(2)°	Fe1 Cl2 2.4324(15)Å	N1 Fe1 Cl2 100.32(12)° N2 Fe1 Cl2 90.46(11)° N4 Fe1 Cl2 88.88(11)° Cl1 Fe1 Cl2 95.45(5)°

Structural Comparison and Analysis

Both complexes exhibit significantly distorted octahedral coordination geometries at the iron center, as evidenced by N-Fe-N bond angles ranging between 70-80°. This distortion arises from the geometric constraints imposed by the five-membered chelate rings formed by the TPA ligand framework. The observed Fe-N bond distances (>2.0 Å) are consistent with a high-spin (S=2) electronic configuration for the Fe (II) centers, characteristic of weak-field ligand environments.

Notably, the nitrile substituents adopt outward orientations relative to the equatorial plane, likely minimizing electronic repulsion between the cyano groups and chloride ligands. In the disubstituted (CN)₂TPAFeCl₂ complex, this steric constraint is particularly pronounced, with the nitrile groups oriented in opposing directions to alleviate intramolecular strain. This structural feature demonstrates the significant conformational influence exerted by multiple nitrile substituents on the overall molecular geometry.

Quantitative Analysis of Trans-Equatorial Deformation

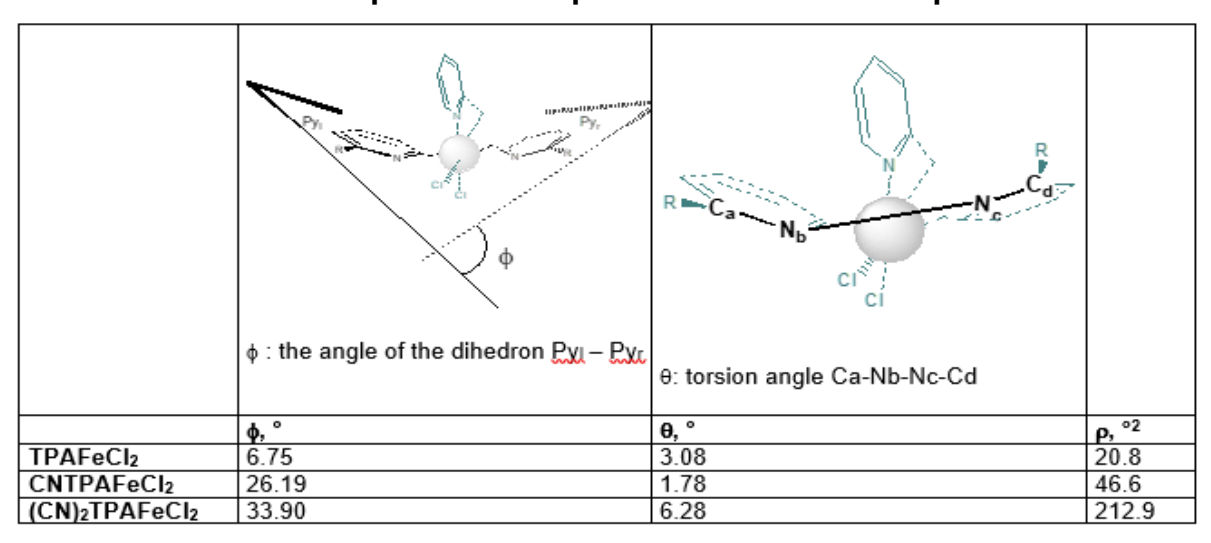
The structural distortion in pseudo-octahedral TPA complexes was quantitatively characterized using the trans-equatorial deformation parameter (ρ), defined as the product of the dihedral angle (φ) between trans-oriented pyridyl rings and their associated torsion angle (θ). Comparative analysis of TPAFeCl₂, CNTPAFeCl₂, and (CN)₂TPAFeCl₂ reveals a pronounced increase in ρ values (Table 4), with the disubstituted complex

E-Publication: Online Open Access

Vol: 68 Issue 10 | 2025 DOI: 10.5281/zenodo.17321958

exhibiting the most significant distortion ($\rho = 212.9^{\circ 2}$ versus $20.8^{\circ 2}$ and $46.6^{\circ 2}$ for the unsubstituted and monosubstituted analogues, respectively).

Table 4: Measured values of ϕ , dihedral angle between two pyridines in trans, of θ : angle of torsion between two pyridines in trans, and $\rho = \phi \times \theta$: trans angular deformation parameter in pseudo-octahedral complexes.



1. Conformational Consequences:

The progressive increase in both ϕ (6.75° \to 33.90°) and θ (3.08° \to 6.28°) across the series demonstrates how nitrile substitution enforces:

- Pyridyl ring twisting (φ)
- Chelate ring puckering (θ)
- o Overall distortion of the coordination sphere

2. Steric Implications:

The observed deformations primarily reflect:

- Repulsive interactions between nitrile electron density and chloride lone pairs
- Geometric constraints imposed by the rigid TPA scaffold
- Cumulative steric demand of multiple nitrile substituents

ISSN: 1673-064X

E-Publication: Online Open Access

Vol: 68 Issue 10 | 2025

DOI: 10.5281/zenodo.17321958

These findings provide quantitative structural evidence for the substantial ligand field perturbations induced by nitrile functionalization, with important implications for understanding the electronic and steric tuning of coordination geometries in substituted TPA complexes.

3. Oxygenation Reactivity of Nitrile-Substituted Iron (II) Complexes

Previous studies have established that unsubstituted TPA-iron complexes undergo direct oxygenation to form symmetric µ-oxo diferric species.

Building upon this foundation, we investigated how electron-withdrawing nitrile substituents influence this reactivity, given their capacity to enhance metal center electrophilicity and potentially accelerate oxygen activation kinetics.

UV-Visible Spectroscopic Monitoring of Oxygenation Kinetics

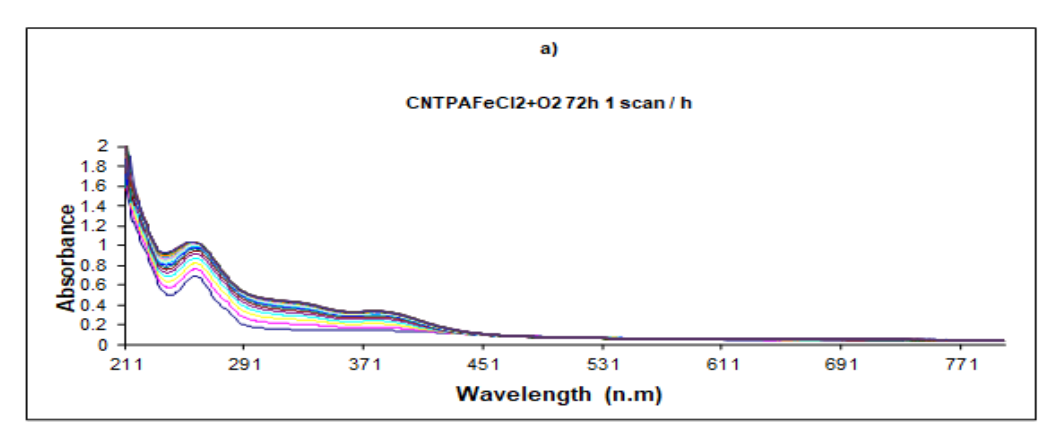
solutions of CNTPAFeCl₂, (CN)₂TPAFeCl₂, and (CN)₃TPAFeCl₂, with reaction progress monitored by UV-vis spectroscopy (Figure 9). Distinct reactivity patterns emerged:

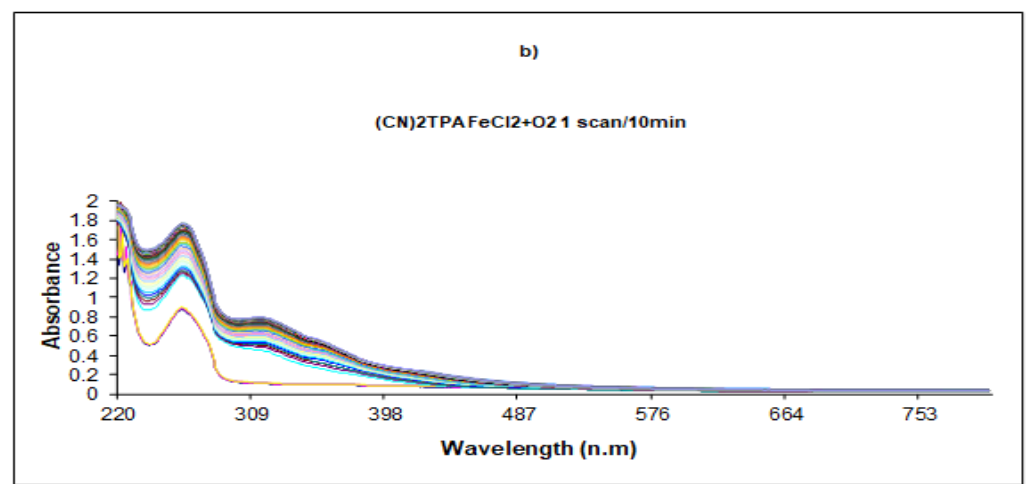
- CNTPAFeCl₂ exhibited gradual conversion over 15 hours, evidenced by a progressive color change to brown. The final spectrum displayed characteristic absorptions at 327 nm and 380 nm, consistent with formation of a symmetric μ-oxo diferric species Figure 9: a).
- 2. (CN)₂TPAFeCl₂ demonstrated biphasic kinetics:
 - Rapid initial phase (complete within 30 minutes)
 - Slower secondary process (4 hours total reaction time) Final absorption bands at 316 nm and 358 nm suggest a μ-oxo bridged structure with intermediate symmetry Figure 9: b).
- 3. **(CN)**₃**TPAFeCl**₂ showed the fastest reactivity:
 - Immediate initial transformation (15 minutes)
 - Subsequent gradual evolution (90 minutes total) Diagnostic bands at 255 nm and 315 nm indicate symmetric μ-oxo diferric product formation Figure 9: c).

E-Publication: Online Open Access

Vol: 68 Issue 10 | 2025

DOI: 10.5281/zenodo.17321958





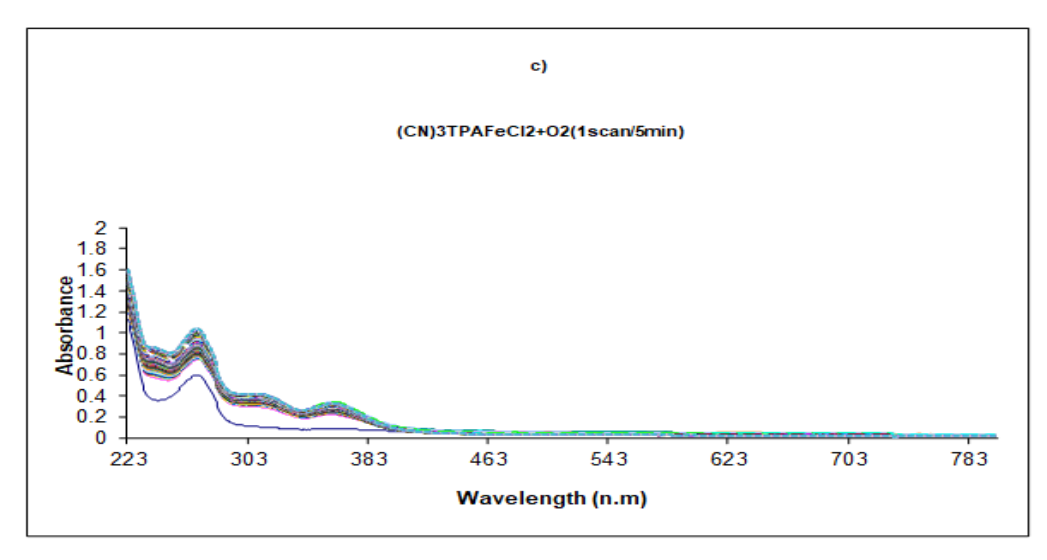


Figure 9: UV-vis tracking of the oxygenation reaction of the complexes: a) CNTPAFeCl₂, b) (CN)2TPAFeCl₂, c) (CN)3TPAFeCl₂.

ISSN: 1673-064X

E-Publication: Online Open Access

Vol: 68 Issue 10 | 2025 DOI: 10.5281/zenodo.17321958

Structure-Reactivity Relationships

The observed kinetic trends correlate strongly with the degree of nitrile substitution:

- Reaction rates increase with additional nitrile groups [(CN)₃TPAFeCl₂ > (CN)₂TPAFeCl₂ > CNTPAFeCl₂]
- Multi-step pathways emerge for di- and tri-substituted complexes
- Final product speciation depends on ligand architecture

	CNTPAFeCl ₂	(CN) ₂ TPAFeCl ₂	(CN) ₃ TPAFeCl ₂
Color change	Red-brown	Red-brown	Chestnut
Color change	15 hours	30 minutes	15 minutes

These findings validate the hypothesis that electron-deficient iron centers (induced by nitrile substitution) enhance oxygenation reactivity.

The spectroscopic evidence further suggests that nitrile loading influences both reaction kinetics and the structural nature of the resulting oxo-bridged products, with intermediate symmetries possible for certain substitution patterns.

This systematic study provides fundamental insights into tuning oxygen activation pathways through rational ligand design.

II. Paramagnetic ¹H NMR Spectroscopic Monitoring of CNTPAFeCl₂ Oxygenation

The oxygenation process of CNTPAFeCl₂ was investigated using ¹H NMR spectroscopy in CD₃CN to elucidate structural and electronic transformations. In the deoxygenated state, the complex exhibits characteristic paramagnetic behavior with resonances dispersed across an extensive chemical shift range (-50 to 160 ppm), consistent with a high-spin Fe (II) center (S = 2).

Upon dioxygen exposure, dramatic spectral changes occur due to formation of a binuclear μ -oxo-bridged Fe (III) species. The emergence of antiferromagnetic coupling between iron centers (S = 5/2 per Fe (III)) through the oxo bridge induces partial diamagnetic character in the system, manifested by:

- 1. Progressive disappearance of paramagnetically-shifted signals
- 2. Appearance of free ligand resonances after 4 hours
- 3. Development of broadened peaks in the 20 to -10 ppm range

Time-dependent spectral evolution (Figure 10) reveals:

- Residual starting material persists after 24 hours
- Complete conversion to the oxo-bridged product occurs by 72 hours
- Final spectrum shows characteristic pseudo-diamagnetic pattern of antiferromagnetically-coupled [Fe (III)-O-Fe (III)] core

E-Publication: Online Open Access

Vol: 68 Issue 10 | 2025

DOI: 10.5281/zenodo.17321958

These observations demonstrate:

- The μ-oxo bridge mediates strong magnetic exchange (J ≈ -100 cm⁻¹)
- Oxygenation proceeds through detectable intermediate states
- Final product retains some paramagnetic broadening due to incomplete spin cancellation

This NMR evidence complements UV-vis data in establishing the oxygenation pathway and final product electronic structure, while providing unique insight into the timescale of binuclear complex formation. The persistence of intermediate signals suggests stepwise oxidation and dimerization kinetics rather than concerted mechanism.

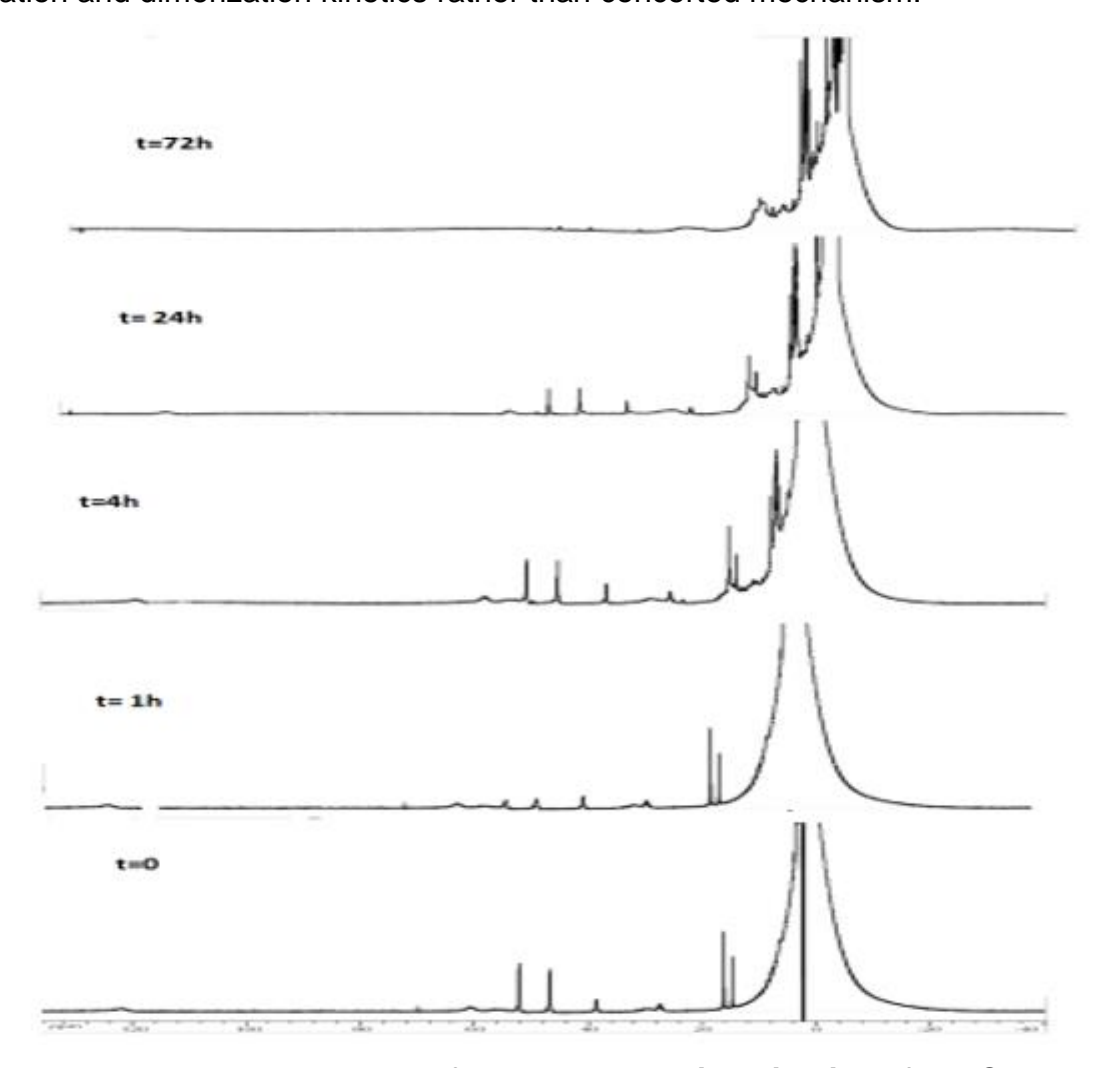


Figure 10: The 1H NMR spectra, for the oxygenation kinetics of the CNTPAFeCl₂ complex at: a) t = 0, b) t = 1h, c) t = 4h, d) t = 24h, e) t = 72h. The stars correspond to the signals of the traces of the starting product.

E-Publication: Online Open Access

Vol: 68 Issue 10 | 2025 DOI: 10.5281/zenodo.17321958

2) Substrate Oxidation Reactivity and Catalytic Performance

The proposed oxygenation mechanism (Figure 11) involves the formation of a highly reactive Fe (IV)-oxo intermediate, which, in the absence of an external substrate, undergoes comproportionation with another Fe(II) complex to yield a μ -oxo diferric species. However, in the presence of a hydrocarbon substrate such as cyclohexane, this high-valent oxo species may instead facilitate oxygen atom transfer, leading to substrate oxidation (e.g., conversion to cyclohexanone).

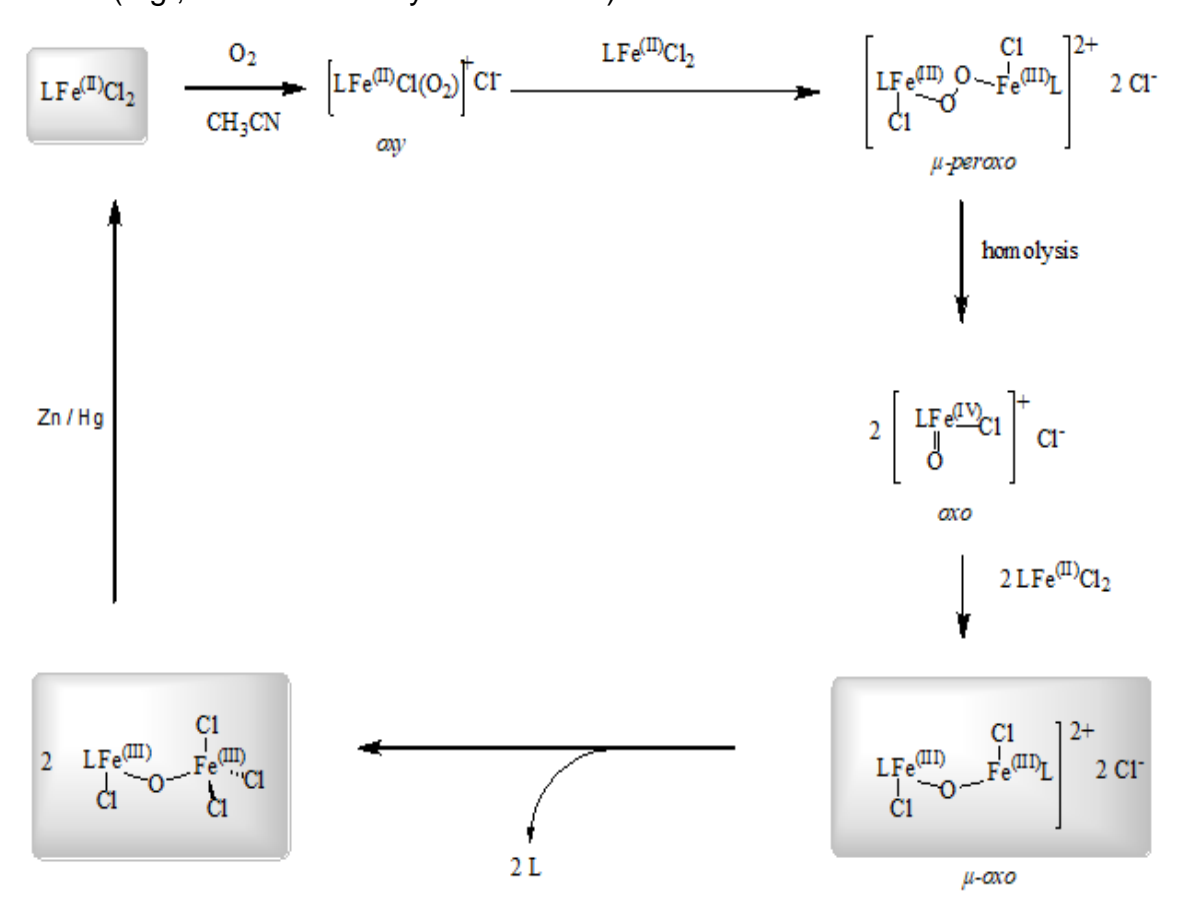


Figure 11: The oxygenation mechanism of the complexes.

To evaluate this hypothesis, catalytic oxygenation experiments were conducted using nitrile-substituted Fe (II) complexes (TPACNFeCl₂, TPACN₂FeCl₂, TPACN₃FeCl₂) under an O_2 atmosphere, with cyclohexane as the substrate and zinc amalgam as a reductant to maintain the Fe (II/III) redox cycle.

The reaction mixture, consisting of the catalyst, cyclohexane, and zinc amalgam in acetonitrile, was oxygenated for 1–2 h, yielding a grayish solution. Acetophenone was introduced as an internal standard prior to filtration through Celite, and the products were analyzed by gas chromatography (GC).

ISSN: 1673-064X

E-Publication: Online Open Access

Vol: 68 Issue 10 | 2025 DOI: 10.5281/zenodo.17321958

GC Analysis and Turnover Number (TON) Determination

The GC chromatograms exhibited distinct retention times for key components:

- **4.1 min**: Solvent (acetonitrile)
- ~4.5 min: Cyclohexane (low-intensity peak)
- **6.6 min**: Cyclohexanone (minor product)
- 11.6 min: Acetophenone (internal standard)

The cyclohexanone concentration was quantified using the relative peak areas:

[cyclohexanone]=1.2×[acetophenone]×Area (cyclohexanone)Area (acetophenone)[cyclohexanone]=1.2×[acetophenone]×Area (acetophenone)Area (cyclohexanone)

The catalytic efficiency was expressed as the turnover number (TON):

TON=[cyclohexanone][catalyst]TON=[catalyst][cyclohexanone]

Comparative Catalytic Performance

The TON values obtained for the different complexes reveal significant variations in reactivity:

Complex	TON
TPAFeCl ₂	8
TPACNFeCl ₂	25
TPACN ₂ FeCl ₂	84
TPACN ₃ FeCl ₂	9

- **-Enhanced Reactivity with Nitrile Substitution**: The disubstituted complex (TPACN₂FeCl₂) exhibited the highest catalytic activity (TON = 84), suggesting an optimal balance between electronic activation and steric accessibility.
 - Electronic vs. Steric Effects: While mono- and di-nitrile substitution improved TON relative to unsubstituted TPAFeCl₂, the tri-nitrile analogue (TPACN₃FeCl₂) showed reduced efficiency, likely due to excessive steric hindrance impeding substrate approach.
 - Comparison with Fluorinated Analogues: The trend aligns with prior studies on fluorinated TPA complexes, where electron-withdrawing groups enhance Fe (IV)=O formation but excessive substitution diminishes reactivity.

These results demonstrate that strategic ligand modification can fine-tune the oxidative capability of Fe (II) catalysts, with TPACN₂FeCl₂ emerging as the most effective system for cyclohexane oxidation under these conditions. Further mechanistic studies are warranted to elucidate the role of nitrile groups in stabilizing high-valent intermediates and facilitating C–H activation [151,152]. This research demonstrates that nitrile-functionalized iron-TPA complexes can be leveraged as a novel class of pro-oxidant cancer therapeutics. Their application hinges on the catalytic activation of molecular

ISSN: 1673-064X

E-Publication: Online Open Access Vol: 68 Issue 10 | 2025

DOI: 10.5281/zenodo.17321958

oxygen (O₂) to generate reactive oxygen species (ROS) directly within cancer cells [153-156]. The therapeutic mechanism exploits the inherent oxidative vulnerability of many cancers. Tumor cells often operate under elevated basal ROS stress, making them particularly susceptible to further oxidative insult.

These complexes catalyze sustained ROS production, overwhelming the cancer cells' antioxidant defenses and inducing lethal damage to DNA and lipids, while theoretically sparing normal cells with more robust redox homeostasis. A key advantage is their functionality in hypoxic tumor microenvironments, where traditional therapies like radiation often fail, as they utilize available O₂. Furthermore, the zinc-mediated redox cycling allows for catalytic, dose-efficient ROS generation.[157]. The disubstituted complex, (CN)₂TPAFeCl₂, exhibits the optimal balance of electronic activation and steric accessibility, making it the most promising candidate. Its enhanced Lewis acidity facilitates rapid O₂ activation without excessive steric hindrance that could impede reactivity. While the article does not specify a single cancer type, this biomimetic strategy is best suited for cancers characterized by oxidative stress and hypoxic regions, such as pancreatic, glioblastoma, and certain resistant solid tumors. The tunability of the ligand platform allows for future optimization to target specific cancer subtypes.

CONCLUSIONS

This research has successfully established a robust platform for the rational design of biomimetic iron complexes through the systematic development and characterization of a novel series of nitrile-functionalized tris(2-pyridylmethyl) amine (TPA) ligands and their corresponding iron (II) complexes. The strategic incorporation of one, two, or three electron-withdrawing nitrile groups at the α-pyridyl position has proven to be a highly effective method for precisely modulating the electronic structure of the metal center. Electrochemical analysis quantitatively demonstrated a consistent, additive increase in ligand oxidation potential of approximately 110 mV per nitrile substituent, unequivocally confirming the strong electron-withdrawing character of the cyano group and its capacity to stabilize the ligand's highest occupied molecular orbital. The profound electronic perturbation induced by nitrile substitution directly translates to significant structural and functional consequences.

Single-crystal X-ray diffraction analyses of CNTPAFeCl₂ and (CN)₂TPAFeCl₂ revealed distinct, progressively distorted pseudo-octahedral geometries. The quantitative assessment using the trans-equatorial deformation parameter (ρ) provided compelling structural evidence of this distortion, which escalates dramatically with increased nitrile loading. This distortion is attributed to steric and electronic repulsions between the nitrile substituents and the chloride ligands, underscoring the intricate interplay between electronic tuning and geometric constraints in substituted TPA complexes. Solution-phase studies, including paramagnetic NMR and conductometry, confirmed the persistence of these neutral, high-spin Fe (II) species in acetonitrile, validating the solid-state structures as relevant to solution reactivity. The core objective of enhancing small-

ISSN: 1673-064X

E-Publication: Online Open Access Vol: 68 Issue 10 | 2025

DOI: 10.5281/zenodo.17321958

molecule activation was decisively met. A clear and direct correlation was established between the ligand-induced electron deficiency at the iron center and the kinetics of dioxygen activation. The oxygenation reactivity increased markedly with the degree of nitrile substitution, with (CN)₃TPAFeCl₂ reacting most rapidly. Spectroscopic monitoring (UV-Vis and ¹H NMR) of these reactions confirmed the formation of μ-oxo diferric species, with the specific product speciation—ranging from symmetric to asymmetric bridged dimers—being influenced by the ligand architecture. This behavior supports a mechanism involving inner-sphere dioxygen coordination, facilitated by the enhanced Lewis acidity of the electron-deficient iron center, rather than an outer-sphere electron transfer pathway. The catalytic proficiency of these complexes was unequivocally demonstrated in the oxidation of cyclohexane to cyclohexanone under a dioxygen atmosphere.

The disubstituted complex, (CN)₂TPAFeCl₂, emerged as the optimal catalyst, achieving a turnover number (TON) of 84, which significantly surpasses the activity of both the parent TPAFeCl₂ (TON = 8) and the trisubstituted analogue (TON = 9). This structureactivity relationship identifies a critical "sweet spot" where the electronic activation for O₂ binding and high-valent Fe (IV)=O intermediate formation is maximized, without introducing excessive steric hindrance that would impede substrate access to the active site. The successful implementation of a zinc amalgam reductant to sustain the catalytic cycle underscores the potential for these systems to function as efficient, recyclable oxidation catalysts. Beyond fundamental catalytic applications, this work pioneers a novel therapeutic paradigm based on catalytic oxygen activation. The developed nitrilefunctionalized iron-TPA complexes function as bioinspired pro-oxidant agents, capable of exploiting tumor-specific vulnerabilities. Their mechanism of action involves the in situ catalytic generation of reactive oxygen species (ROS), inducing lethal oxidative stress in cancer cells. This strategy offers several transformative advantages: (1) **Selectivity**, leveraging the inherently elevated basal ROS levels in cancer cells to create a therapeutic window; (2) Hypoxia Compatibility, as their mechanism relies on available O2, making them potentially effective against hypoxic tumors resistant to radiation and many conventional chemotherapies; and (3) Catalytic Efficiency, enabled by redox cycling, which allows for sustained ROS production at low therapeutic doses.

The lead candidate, (CN)₂TPAFeCl₂, with its optimal balance of reactivity and stability, is particularly promising for this application. This study provides a comprehensive structure-property relationship framework for a new class of electron-deficient iron complexes. It validates ligand electronic modulation as a powerful strategy for enhancing small-molecule activation and catalytic oxidation. Furthermore, it introduces a groundbreaking, biomimetic approach to cancer therapy that operates through catalytic oxidative stress. The insights gained into the interplay of electronic and steric effects provide a clear roadmap for the design of next-generation oxidation catalysts and therapeutic agents. Future work will focus on conjugating these complexes with tumor-targeting moieties to enhance specificity and rigorously evaluating their efficacy and safety in advanced preclinical models, thereby translating this innovative chemical design into a potent therapeutic strategy.

ISSN: 1673-064X

E-Publication: Online Open Access

Vol: 68 Issue 10 | 2025

DOI: 10.5281/zenodo.17321958

References

- 1) Machkour A, Thallaj NK, Benhamou L, Lachkar M, Mandon D.Chemistry. 2006 Aug 25;12(25):6660-8. P. https://doi.org/10.1002/chem.200600276.
- Thallaj, N., Machkour, A., Mandon, D., Welter, R., New. J. Chem., 2005, 29, 1555 1558. https://doi.org/10.1039/B512108F
- Thallaj NK, Rotthaus O, Benhamou L, Humbert N, Elhabiri M, Lachkar M, Welter R, Albrecht-Gary AM, Mandon D. Chemistry

 –A European Journal 14 (22), 6742-6753. 2008.
 https://doi.org/10.1002/chem.200701967
- Wane A, Thallaj NK, Mandon D. Chemistry. 2009 Oct 12;15(40):10593-602. P10594-10595-10595. https://doi.org/10.1002/chem.200901350
- 5) Thallaj NK, Orain PY, Thibon A, Sandroni M, Welter R, Mandon D. Inorg Chem. 2014 Aug 4;53(15):7824-36. P7826-7828. https://doi.org/10.1021/ic500096h
- 6) N. K. Thallaj, J. Przybilla, R. Welter and D. Mandon, J. Am. Chem. Soc. 2008, 130, 2414-2415. https://doi.org/10.1021/ja710560g
- 7) N. K. Thallaj, D. Mandon and K. A. White, Eur. J. of Inorg. Chem., 2007, 44–47. https://doi.org/10.1002/ejic.200600789.
- 8) Thallaj, N.; International journal of applied chemistry and biological sciences 2021, 2 (4), 65-77. https://identifier.visnav.in/1.0001/ijacbs-21f-07003/
- Thallaj, N. Review of a Few Selected Examples of Intermolecular Dioxygenases Involving Molecular Oxygen and Non-Heme Iron Proteins. Int. J. Adv. Parmacutical Sci. Res. (IJAPSR) (2023)., 3, 1-18. DOI: 10.54105/ijapsr.C4011.023223
- 10) L. Labban, M. Kudsi, Z. Malek, N. Thallaj; Advances in Medical, Dental and Health Sciences, 2020,3, 3,45-48. DOI: 10.5530/amdhs.2020.3.11
- 11) L. Labban, N. Thallaj, M. Al Masri; Journal of Advanced Research in Food Science and Nutrition, 2020,3,1,34-41. doi: 10.11648/j.wjfst.20190304.11. http://www.florajournal.com
- 12) L. labban; N. thallaj; A. labban; archives of medicine, 2020, 12, 2:8, 1-5. DOI: 10.36648/1989-5216.12.2.309
- 13) L. Labban, N. Thallaj, Z. Malek; Journal of Medical Research and Health Sciences, 2019, 2, 11, 784-787. https://doi.org/10.15520/jmrhs.v2i11.128
- A. Abbood, S.A. Malik.D. aldiab,H. H.Ali, N.Thallaj. Investigation of the charge variant profile of noncleavable conjugated antibodies, Research J. Pharm. and Tech. 2025; 18(1) 185-190. DOI: 10.52711/0974-360X.2025.00028.
- 15) Y. alhomush, Z. malek, A. Abboud, N.Thallaj, Research Journal of Pharmacy and Technology, 2022, 15, 10. doi: 10.52711/0974-360X.2022.00794.
- 16) A.Abbood, Z.Malek, N.Thallaj. 2022 15, 11, 4935-4939. Research Journal of Pharmacy and Technology. doi: 10.52711/0974-360X.2022.00829.
- 17) Thallaj, N; agha, M. I, H; nattouf; A.H; katib, CH; karaali, A; Moustapha, A; Labban L;open access library journal, 2020,7,5,1-21. https://doi.org/10.4236/oalib.1106302.
- 18) N.Thallaj. Indian journal of advanced chemistry, 2021. 1, 2, 20-26. DOI: 10.54105/ijac. B2009.101221
- 19) N.Thallaj. Indian journal of advanced chemistry, 2022. 2, 2, 1-11. DOI: 10.54105/ijac. D2015.102222
- 20) N.Thallai, Indian journal of advanced chemistry, 2, 1, 2022. 5-9. DOI: 10.54105/ijac.C2012.041322
- 21) N.Thallaj. Indian journal of advanced chemistry, 2, 1, 2022. 10-14. DOI: 10.54105/ijac.C2013.041322

ISSN: 1673-064X

E-Publication: Online Open Access

Vol: 68 Issue 10 | 2025

DOI: 10.5281/zenodo.17321958

- 22) N.Thallaj.Xi'an ShiyouDaxueXuebao (ZiranKexue Ban)/ Journal of Xi'an Shiyou University, Natural Sciences Edition.2022.65, 06. 289-301. DOI:10.17605/OSF.IO/W8RS5
- 23) N.Thallaj. Xi'an ShiyouDaxueXuebao (ZiranKexue Ban)/ Journal of Xi'an Shiyou University, Natural Sciences Edition.2022.65, 06. 313-328. DOI:10.17605/OSF.IO/K8RFE
- 24) Z. MALEK, A. ABBOOD, N. THALLAJ. Xi'an ShiyouDaxueXuebao (ZiranKexue Ban)/ Journal of Xi'an Shiyou University, Natural Sciences Edition.2022.65, 06. 302-312. DOI:10.17605/OSF.IO/K56XY
- 25) N.Thallaj. 2022. 65, 7, 169-184. Xi'an Shiyou Daxue Xuebao (Ziran Kexue Ban)/Journal of Xi'an Shiyou University, Natural Sciences Edition. DOI:10.17605/OSF.IO/7F23D
- 26) N.Thallaj. 2022. 65, 7, 110-142. Xi'an Shiyou Daxue Xuebao (Ziran Kexue Ban)/Journal of Xi'an Shiyou University, Natural Sciences Edition. DOI:10.17605/OSF.IO/KZRDJ
- 27) N Thallai, (2023). 44, (6),21-29. Tishreen University Journal-Medical Sciences Series.
- 28) N.Thallaj. International Journal of Advanced Pharmaceutical Sciences and Research (IJAPSR) 2022. 2, 3,1-28. DOI: 10.54105/ijapsr.C4018.042322
- 29) N.Thallaj. International Journal of Advanced Pharmaceutical Sciences and Research (IJAPSR) 2022. 2, 4,1-15. DOI: 10.54105/ijapsr.C4016.062422
- 30) N.Thallaj. International Journal of Advanced Pharmaceutical Sciences and Research (IJAPSR) 2023. 3, 2,1-18. DOI: 10.54105/ijapsr.C4016.062422
- 31) N.Thallaj. International Journal of Advanced Pharmaceutical Sciences and Research (IJAPSR) 2022. 2, 6,1-12. DOI: 10.54105/ijapsr.C4015.102622
- 32) N.Thallaj. International Journal of Advanced Pharmaceutical Sciences and Research (IJAPSR) 2023. 3, 3,1-10. DOI: 10.54105/ijapsr.C4012.043323
- N.Thallaj. International Journal of Advanced Pharmaceutical Sciences and Research (IJAPSR) 2024.
 1,32-52. DOI: 10.54105/ijapsr. A4036.124123
- 34) N.Thallaj. International Journal of Advanced Pharmaceutical Sciences and Research (IJAPSR) 2024. 4, 5,29-49. DOI: 10.54105/ijapsr. E4049.04050824
- 35) N.Thallaj. International Journal of Advanced Pharmaceutical Sciences and Research (IJAPSR) 2024.4, 4,7-21. DOI: 10.54105/ijapsr. D4042.04040624
- 36) N.Thallaj. International Journal of Advanced Pharmaceutical Sciences and Research (IJAPSR) 2024.4, 6,7-27. DOI: 10.54105/ijapsr. F4054.04061024
- 37) N.Thallaj. International Journal of Advanced Pharmaceutical Sciences and Research (IJAPSR) 2024.4, 6,33-48. DOI: 10.54105/ijapsr. F4055.04061024
- 38) Besherb S, Alallan L, Hassan Agha MA, Alshamas I, Thallaj N. Influence of soil salinity on the chemical composition of essential oil of Rosmarinus Officinalis in Syria, Research J. Pharm. and Tech. 2024; 17(5). DOI: 10.52711/0974-360X.2024.00358
- 39) Thallaj, N. (2024). Advancements in Pharmaceutical Science: Synthesis and Application of Molecular Cages Integrating N-Heterocyclic Carbenes for Enhanced Stability and Functionality. International Journal of Advanced Pharmaceutical Sciences and Research (IJAPSR), 5(1), 6-19. DOI: https://doi.org/10.54105/ijapsr.A4063.05011224
- 40) Ayat Abbood, Hassan Hadi Ali, Samir Azzat Malik, Dima AlDiab, Nasser Thallaj. Investigation of the Charge Variant Profile of Non-cleavable Conjugated Antibodies. Research Journal of Pharmacy and Technology. 2025;18(1):185-0. doi: 10.52711/0974-360X.2025.00028

ISSN: 1673-064X

E-Publication: Online Open Access

Vol: 68 Issue 10 | 2025 DOI: 10.5281/zenodo.17321958

- 41) Thallaj, N. Analyzing Charge Variant Profiles of Monoclonal Antibodies Conjugated to Cytotoxic Agents. International Journal of Advanced Pharmaceutical Sciences and Research (IJAPSR), Volume-4 Issue-3, april 2025, pages 20-26. DOI:10.54105/ijapsr.C4071.05030425
- 42) Thallaj, N. Biomimetic Synthesis and Phytochemical Analysis of Lodopyridone: Insights into 4-Pyridone Derivatives and Thiopeptide Antibiotic. Journal of Advanced Pharmaceutical Sciences and Research (IJAPSR), Volume-4 Issue-3, april 2025, pages 9-19. DOI: 10.54105/ijapsr. B4069.05030425
- 43) Mousa Al Khleif, Nour Alhuda Alzoubi, Ghassan Shannan, Zeina S Malek, Nasser Thallaj*. Exploring Circadian Rhythms:A Comprehensive Study on Sleep Patterns and Disorders in Syrian Society. Am J Biomed Sci & Res. 2025 26(2) AJBSR.MS.ID.003416, DOI:10.34297/AJBSR.2025.26.003416.
- 44) Ranim Abdul Rahman, Louai Alallan, Ahmed Khalid Aldhalmi, Nasser Thallaj. Separation, Determination, and Potential Application of Active Compounds in Porosopis cineraria: A Comprehensive Analysis. Research Journal of Pharmacy and Technology. 2025;18(4):1604-0. doi: 10.52711/0974-360X.2025.00230
- 45) Dalia Aboufakher, Rita Zeinaldin, Racha Khatib, Rawa Khreit, Mohamed Sami Joha, Nasser Thallaj. Prevalence and AntibioticResistance Patterns of Multidrug-Resistant Gram-Negative Bacilli in Hospitalized Patients in Sweida, Syria. Am J Biomed Sci & Res. 2025 26(3) AJBSR.MS.ID.003436, DOI: 10.34297/AJBSR.2025.26.003436.
- 46) Khatib O, Alshimale T, Alsaadi A, Thallaj N. The Global Impact of HIV: A Comprehensive Review. IJAPSR, vol. 4, no. 3, pp. 6–19, Apr. 2024. doi: 10.54105/ijapsr.C4040.04030424.
- 47) Samer alkhoury, Rasha Kateeb, Rawa Akasha and Nasser Thallaj*. Analysis of Crocin Content in Saffron (Crocuss ativus L) Cultivated in Syria Using Liquid Chromatography-Mass Spectrometry. Am J Biomed Sci & Res. 2025 26(3) AJBSR.MS.ID.003443, DOI: 10.34297/AJBSR.2025.26.003443.
- 48) Thallaj, N. (2022). Design and Synthesis Ligands Tetradents Substituted with Halogenes in α- Position and Conjugation with Riboflavin (Bioconjugates): Conjugate ligands Type TPA's with Flavonoids as un–Electron Mediator. Biomedicine and Chemical Sciences, 1(2), 47–56, https://doi.org/10.48112/bcs.v1i2.85.
- 49) Thallaj, N., Alrasho, J. F., & Sofi, F. K. (2024). Advancements in Antiviral Therapeutics: A Comprehensive Review of Hepatitis C Virus and Novel Flavone Leads. International Journal of Advanced Pharmaceutical Sciences and Research (IJAPSR), 5(1), 28-40.
 - DOI:https://doi.org/10.54105/ijapsr.A4064.05011224.
- 50) Thallaj, N. Biomimetic Synthesis and Phytochemical Analysis of Lodopyridone: Insights into 4-Pyridone Derivatives and Thiopeptide Antibiotics. International Journal of Advanced Pharmaceutical Sciences and Research (IJAPSR), Volume-5 Issue-3, April 2025, pages 9-19. DOI: 10.54105/ijapsr. B4069.05030425.
- 51) Labban, L., M. Kudsi, Z. Malek, and N. Thallaj. "Advances in Medical, Dental and Health Sciences, 2020, 3, 3, 45-48." DOI: https://doi. org/10.5530/amdhs 11 (2020).
- 52) Thallaj, N. (2023). A Brief Overview of the General Characteristics and Reactivity Towards Dioxygen of the Ferrous Tris (2-Pyridylmethyl Amine) Series Complexes is Presented. International Journal of Advanced Pharmaceutical Sciences and Research (IJAPSR), 3(3), 1-18.
- 53) Thallaj, N. (2024). Advancements in Pharmaceutical Science: Synthesis and Application of Molecular Cages Integrating N-Heterocyclic Carbenes for Enhanced Stability and Functionality. International Journal of Advanced Pharmaceutical Sciences and Research (IJAPSR), 5(1), 6-19

ISSN: 1673-064X

E-Publication: Online Open Access

Vol: 68 Issue 10 | 2025

DOI: 10.5281/zenodo.17321958

- 54) Thallaj, N. (2024). Conductive Nanocomposites Based on Graphene and Natural Polymers. International Journal of Advanced Pharmaceutical Sciences and Research (IJAPSR), 4(6), 7-27
- 55) Thallaj, N. (2022). Review of Calixarene-Derivatives in Transition Metal Chemistry. International Journal of Advanced Pharmaceutical Sciences and Research (IJAPSR), 2(3), 1-30.
- 56) Thallaj, N. (2024). Advancements in Peptide Vectors for Cancer Therapy and Tumor Imaging: A Comprehensive Review. International Journal of Advanced Pharmaceutical Sciences and Research (IJAPSR), 4(5), 29-49. DOI: 10.54105/ijapsr. E4049.04050824.
- 57) Thallaj, N., ali Hamad, D. H., Batieh, N. A., & Saker, G. A. (2023). A Review of Colon Cancer Treatment using Photoactive Nanoparticles. International Journal of Advanced Pharmaceutical Sciences and Research (IJAPSR), 3(4), 1-32. DOI:10.54105/ijapsr. D4022.063423
- 58) Ghassan Shannan, Zeina S Malek and Nasser Thallaj*. Advancements in Protein Synthesis: Triazole Multi-Ligation and Cycloadditions for Pharmaceutical Applications. Am J Biomed Sci & Res. 2025 26(5) AJBSR.MS.ID.003481, DOI: 10.34297/AJBSR.2025.26.003481.
- 59) Channan, G. (2018). Communicable diseases in the Mediterranean region. EJIFCC, 29(3), 164.
- 60) Shannan, G. (2011, May). Tuberculosis In the Afcb Countries; Re-Emerging Disease. In Clinical Chemistry and Laboratory Medicine (Vol. 49, Pp. S41-S41). Genthiner Strasse 13, D-10785 Berlin, Germany: Walter De Gruyter & Co.
- 61) Channan, G. M. (1977). Studies of vitamin D hydroxylation in chronic renal failure.
- 62) Aldakhoul, M., Sleman, S., Alragheb, N., Alfarwan, M., Alallan, L., Shubber, Z. I., & Thallaj, N. (2024). Phytochemical Composition and Health Benefits of Pumpkin. Research Journal of Pharmacy and Technology, 17(10), 4915-4921.
- 63) Khabbazeh, Sally, Saly Alhaddad, Yazan Kiwan, Louai Alallan and Nasser Thallaj. "The Benefits of Jujube: Extracting Phenols and Saponins for Medicinal and Nutritional Uses." Azerbaijan Pharmaceutical and Pharmacotherapy Journal 23, no. 4 (2024): 1-7.
- 64) Nasser Thallaj, Dalia Aboufakher, Rita Zeinaldin, Rawa Khreit, Racha KhatibPrevalence and Antibiotic Resistance Patterns of Multidrug-Resistant Gram-Negative Bacilli in Hospitalized Patients in Sweida, Syria. FJHMS 2025, 1 (1), 70-78.
- 65) Thallaj, Dr N. "Review of Calixarene-Derivatives in Transition Metal Chemistry." International Journal of Advanced Pharmaceutical Sciences and Research 2.3 (2022): 1-28.
- 66) Ghassan Shannan, Zeina S Malek and Nasser Thallaj*. Advances in Supported Synthesis of Oligosaccharides Using Thioglycoside Donors. Am J Biomed Sci & Res. 2025 27(1) AJBSR.MS.ID.003528, DOI: 10.34297/AJBSR.2025.27.003528.
- 67) Ghassan Shannan, Zeina S Malek and Nasser Thallaj*. Bioinspired Iron (III) Complexes: Catalysts for Sustainable Oxygen Atom Transfer Reactions. Am J Biomed Sci & Res. 2025 27(1) AJBSR.MS.ID.003516, DOI: 10.34297/AJBSR.2025.27.003516.
- 68) Ghassan Shannan, Zeina S Malek and Nasser Thallaj*. Endosulfatases: Promising Therapeutic Targets in Cancer and Inflammatory Diseases. Am J Biomed Sci & Res. 2025 27(1) AJBSR.MS.ID.003523, DOI: 10.34297/AJBSR.2025.27.003523.
- 69) Samer alkhoury, Rasha Kateeb, Rawa Akasha and Nasser Thallaj*. Analysis of Crocin Content in Saffron (Crocus sativus L) Cultivated in Syria Using Liquid Chromatography-Mass Spectrometry. Am J Biomed Sci & Res. 2025 26(3) AJBSR.MS.ID.003443, DOI: 10.34297/AJBSR.2025.26.003443

ISSN: 1673-064X

E-Publication: Online Open Access

Vol: 68 Issue 10 | 2025 DOI: 10.5281/zenodo.17321958

70) Dalia Aboufakher, Rita Zeinaldin, Racha Khatib, Rawa Khreit, Mohamed Sami Joha, Nasser Thallaj. Prevalence and Antibiotic Resistance Patterns of Multidrug-Resistant Gram-Negative Bacilli in Hospitalized Patients in Sweida, Syria. Am J Biomed Sci & Res. 2025 26(3) AJBSR.MS.ID.003436, DOI: 10.34297/AJBSR.2025.26.003436

- 71) Ghassan Shannan, Zeina S Malek and Nasser Thallaj. Advancements in Monomolecular Multimodal Platforms for Cancer Theranostics. Am J Biomed Sci & Res. 2025 27(3) AJBSR.MS.ID.003569, DOI: 10.34297/AJBSR.2025.27.003569.
- 72) Ahmed Alawadd, Ahmed Aldyry, Rasha Khatib, Rawa Akasha, Mohamed Sami Joha, et al. Serological prevalence of Brucella at the livestock-human interface in northeast of Deir al-Zor in Syria. Am J Biomed Sci & Res. 2025 28(2) AJBSR.MS.ID.003660, DOI: 10.34297/AJBSR.2025.28.003660.
- 73) Mouhmad Anwar Ahmeed, Maya Moeen Issa, Ibrahim Al Tamr, Ghassan Shannan and Nasser Thallaj*. Prevalence andAntibiotic Resistance Patterns of Urinary Tract Infections in Syrian Patients: A Comprehensive Analysis. Am J Biomed Sci & Res. 2025 28(1) AJBSR.MS.ID.003646, DOI: 10.34297/AJBSR.2025.28.003646
- 74) Malek, Z.S.; Journal of AlBaath University 2018, 40(4), 39-62.
- 75) Malek, Z.S.; Tishreen University Journal for Research and Scientific Studies, 2018, 40.
- 76) ZS Malek, LM Labban; International Journal of Neuroscience, 2021,131(12), 1155-1161.
- 77) ZS Malek, LM Labban; Journal of current research in physiology and pharmacology, 2020, 4, (1),1-5.
- 78) L.M. Labban, M. M. Alshishkli, A. Alkhalaf, Z. Malek; J. Adv. Res. Dent. Oral Health, 2017, 2(3&4), 1-4.
- 79) L Labban, ZS Malek, Open Access Library Journal, 2018, 5 (07), 1-11.
- 80) L Labban, ZS Malek, Ann Food Nutr Res J. 2019,1,1
- 81) Malek, Z.S.; Labban, L.; The International Journal of Neuroscience, 2020, 1-7.
- 82) Malek, Z.S.; Labban, L.; European Journal of Pharmaceutical and Medical Research 2019, 6(11), 527-532.
- 83) L. Labban, N. Thallaj, Z. Malek; Journal of Medical Research and Health Sciences, 2019, 2, 11, 784-787.
- 84) 65-77.
- 85) L. Labban, N. Thallaj, Z. Malek; International Journal of Medical Studies, 2020, 5, No 12, 23-36.
- 86) L. Labban, M. Kudsi, Z. Malek, N. Thallaj; Advances in Medical, Dental and Health Sciences, 2020,3, 3,45-48.
- 87) Z. MALEK,2022. 65, 7, 143-152. Xi'an Shiyou Daxue Xuebao (Ziran Kexue Ban)/Journal of Xi'an Shiyou University, Natural Sciences Edition. DOI:10.17605/OSF.IO/2UNHK
- 88) Besherb S, Alallan L, Hassan Agha MA, Alshamas I, Thallaj N. Influence of soil salinity on the chemical composition of essential oil of Rosmarinus Officinalis in Syria, Research J. Pharm. and Tech. 2024; 17(5). DOI: 10.52711/0974-360X.2024.00358
- 89) Ayat Abbood, Hassan Hadi Ali, Samir Azzat Malik, Dima AlDiab, Nasser Thallaj. Investigation of the Charge Variant Profile of Non-cleavable Conjugated Antibodies. Research Journal of Pharmacy and Technology. 2025;18(1):185-0. doi: 10.52711/0974-360X.2025.00028
- 90) Khabbazeh, S., Alhaddad, S., Kiwan, Y., Alallan, L., & Thallaj, N. (2024). The Benefits of Jujube: Extracting Phenols and Saponins for Medicinal and Nutritional Uses. Azerbaijan Pharmaceutical and Pharmacotherapy Journal, 23, 1-7.

ISSN: 1673-064X

E-Publication: Online Open Access

Vol: 68 Issue 10 | 2025 DOI: 10.5281/zenodo.17321958

91) SHANNAN, Ghassan; MALEK, Zeina S.; THALLAJ, Nasser. Advancements in Protein Synthesis: Triazole Multi-Ligation and Cycloadditions for Pharmaceutical Applications.

- 92) SHANNAN, Ghassan; MALEK, Zeina S.; THALLAJ, Nasser. Advancements in Protein Synthesis: Triazole Multi-Ligation and Cycloadditions for Pharmaceutical Applications.
- 93) THALLAJ, Nasser. A Brief Overview of the General Characteristics and Reactivity Towards Dioxygen of the Ferrous Tris (2-Pyridylmethyl Amine) Series Complexes is Presented. International Journal of Advanced Pharmaceutical Sciences and Research (IJAPSR), 2023, 3.3: 1-18.
- 94) NASSER, K. THALLAJ; MANDON, DOMINIQUE; KRISTEN, A. WHITE:" The Design of Metal Chelates with a Biologically Related Redox-Active Part: Conjugation of Riboflavin to Bis (2-pyridylmethyl) amine Ligand and Preparation of a Ferric Complex. EUROPEAN JOURNAL OF INORGANIC CHEMISTRY, 2007, 2007.1: 2007-01.
- 95) THALLAJ, Dr N. Review of Calixarene-Derivatives in Transition Metal Chemistry. International Journal of Advanced Pharmaceutical Sciences and Research, 2022, 2.3: 1-28.
- 96) THALLAJ, Nasser. تاقتشم قبلخت 1، 3، 4-قدعاسمب نيديلوزايث، لوزايداسكوا فيوركياملا. Tishreen University Journal-Medical Sciences Series44, 2022, 1: 59-77.
- 97) ALDAKHOUL, Majd, et al. Phytochemical Composition and Health Benefits of Pumpkin. Research Journal of Pharmacy and Technology, 2024, 17.10: 4915-4921.
- 98) THALLAJ, N. Design and Synthesis of Ligands Tetra dents Substituted with Halogens in α - α - α - α - α -Position and Conjugation with Riboflavin (Bioconjugates): Conjugate ligands Type TPA's with Flavonoids as an Electron Mediator. Biomedicine and Chemical Sciences, 2022, 1.2: 47-56.
- 99) ABOUFAKHER, Dalia, et al. Prevalence and AntibioticResistance Patterns of Multidrug-Resistant Gram-Negative Bacilli in Hospitalized Patients in Sweida, Syria. Am J Biomed Sci & Res, 2025, 26.3.
- 100) SHANNAN, Ghassan; MALEK, Zeina S.; THALLAJ, Nasser. A Review of Antibiotic-Induced Drug Allergies: Mechanisms, Prevalence, And Future Perspectives. European Journal of Biomedical and Pharmaceutical Sciences (EJBPS), 2025, 12.4: 387-399.
- 101) THALLAJ, Nasser. نخليق مشتقات 1، 3، 4-أوكساديازول، ثيازوليدين بمساعدة المايكرويف. Latakia University Journal-Medical Sciences Series, 2022, 44.1: 59-77.
- 102) THALLAJ, Nasser; ABBOOD, Ayat. الشحنة لأضداد وحيدة iclef معايرات الشحنة لأضداد وحيدة Latakia University Journal-Medical Sciences Series, 2023, 45.2: 47-57.
- 103) ALSHHADA, Neamah Omar; ALHAMDO, Haya Asmail; THALLAJ, Nasser. A Review Study of Proline-Derived Paclitaxel as Treatment Anti Cancers. Int. J. Pharm. Sci. Res. 2023, 4: 32-52.
- 104) THALLAJ, Nasser. Biomimetic Synthesis and Phytochemical Analysis of Lodopyridone: Insights into 4-Pyridone Derivatives and Thiopeptide Antibiotic. Journal of Advanced Pharmaceutical Sciences and Research (IJAPSR), 2025, 4.3: 9-19.
- 105) THALLAJ, Nasser. Analyzing Charge Variant Profiles of Monoclonal Antibodies Conjugated to Cytotoxic Agents. International Journal of Advanced Pharmaceutical Sciences and Research (IJAPSR), 2025, 4.3: 20-26.
- 106) THALLAJ, Nasser, et al. Studying the efficacy of the plant extract of Tetracera scandens as an antidiabetic treatment. Latakia University Journal-Medical Sciences Series, 2023, 45.1: 33-44.
- 107) DAYOUB, Leen; ALKUDDSI, Yanal; THALLAJ, Nasser. Investigating the interaction between some of Bipolaris sorokiniana's toxins and the $G\alpha$ Subunit of the Wheat G-Protein using bioinformatics tools. University of Thi-Qar Journal of agricultural research, 2023, 12.1: 181-200.

ISSN: 1673-064X

E-Publication: Online Open Access

Vol: 68 Issue 10 | 2025 DOI: 10.5281/zenodo.17321958

108) THALLAJ, Nasser. Advancements in Peptide Vectors for Cancer Therapy and Tumor Imaging: A Comprehensive Review. International Journal of Advanced Pharmaceutical Sciences and Research (IJAPSR), 2024, 4.5: 29-49.

- 109) THALLAJ, Nasser. Advancements in Inverse-Electron-Demand Diels-Alder Cycloaddition of 2-Pyrones: Mechanisms, Methodologies. International Journal of Advanced Pharmaceutical Sciences and Research (IJAPSR), 2024, 4.6: 33-48.
- 110) ABBOOD, Ayat, et al. Investigation of the Charge Variant Profile of Non-cleavable Conjugated Antibodies. Research Journal of Pharmacy and Technology, 2025, 18.1: 185-190.
- 111) THALLAJ, N. (2023). 44, (6), 21-29. Tishreen University Journal-Medical Sciences Series.
- 112) THALLAJ, Nasser. Conductive Nanocomposites Based on Graphene and Natural Polymers. International Journal of Advanced Pharmaceutical Sciences and Research (IJAPSR), 2024, 4.6: 7-27.
- 113) ABBOOD, A., et al. 15, 10, 4727-4732. Research Journal of Pharmacy and Technology, 2022.
- 114) THALLAJ, Nasser. The Construction of Multichromophoric Assemblages: A Booming Field. International Journal of Advanced Pharmaceutical Sciences and Research (IJAPSR), 2024, 4.4: 7-21.
- 115) THALLAJ, Nasser. HPLC method validation for determination of pentoxifylline in pharmaceutical dosage forms. Indian journal of advanced chemistry, 2022, 2.1: 5-9.
- 116) THALLAJ, N.; ABBOOD, A. Comparison between chromatofocusing and icIEF charge variant profiles of unconjugated monoclonal antibodies and their drug conjugates. Tishreen University Journal-Medical Sciences Series, 2023, 45.2: 47-57.
- 117) THALLAJ, Nasser. Characterization of charge heterogeneity of antibody-drug conjugate by anion-exchange chromatofocusing. Latakia University Journal-Medical Sciences Series, 2022, 44.6: 21-29
- 118) ALRASHO, Juan Farhad; SOFI, Farhad Khalil; THALLAJ, Nasser. Advancements in Antiviral Therapeutics: A Comprehensive Review of Hepatitis C Virus and Novel Flavone Leads. International Journal of Advanced Pharmaceutical Sciences and Research (IJAPSR), 2024, 5: 28-40.
- 119) THALLAJ, Nasser. Design and Synthesis Ligands Tetradents Substituted with Halogenes in α-Position and Conjugation with Riboflavin (Bioconjugates): Conjugate ligands Type TPA's with Flavonoids as un–Electron Mediator. Biomedicine and Chemical Sciences, 2022, 1.2: 47-56.
- 120) BESHERB, S., et al. Influence of soil salinity on the chemical composition of essential oil of Rosmarinus Officinalis in Syria, Research J. Pharm. and Tech, 2024, 17.5.
- 121) WANE, A.; THALLAJ, N. K.; MANDON, D. The Reactivity of Molecular Dioxygen on a Series of Isostructural Dichloroferrous Complexes with Tripodal Tetraamine Ligands: General Access to μoxo Diferric Complexes, and Effect of α-Fluorination on the Kinetics of the Reaction. Chemistry A European Journal, 2008, 14.22: 6742-6753.
- 122) THALLAJ, Nasser, et al. Evaluation of antimicrobial activities and bioactive compounds of different extracts related to syrian traditional products of damask rose (Rosa damascena). Open Access Library Journal, 2020, 7.05: 1.
- 123) LABBAN, L., et al. Advances in Medical, Dental and Health Sciences, 2020, 3, 3, 45-48. DOI: https://doi. org/10.5530/amdhs, 2020, 11.
- 124) THALLAJ, Nasser. A Brief Overview of the General Characteristics and Reactivity Towards Dioxygen of the Ferrous Tris (2-Pyridylmethyl Amine) Series Complexes is Presented. International Journal of Advanced Pharmaceutical Sciences and Research (IJAPSR), 2023, 3.3: 1-18.

ISSN: 1673-064X

E-Publication: Online Open Access

Vol: 68 Issue 10 | 2025 DOI: 10.5281/zenodo.17321958

125) THALLAJ, N.; VASHISHTHA, E. A Review of Bis-Porphyrin Nucleoside Spacers for Molecular Recognition. FMDB Transactions on Sustainable Health Science Letters, 2023, 1.2: 54-69.

- 126) THALLAJ, Nasser. Detecting Antioxidant Behavior for Phenolic Content of Some Beauty Care Creams in Syrian Market. Indian journal of advanced chemistry, 2024, 2.1: 10-14.
- 127) WANE, Amadou; THALLAJ, Nasser K.; MANDON, Dominique. Biomimetic Interaction between Fell and O2: Effect of the Second Coordination Sphere on O2 Binding to Fell Complexes: Evidence of Coordination at the Metal Centre by a Dissociative Mechanism in the Formation of μ-Oxo Diferric Complexes. Chemistry–A European Journal. 2009. 15.40: 10593-10602.
- 128) ABBOOD, A.; MALEK, Z.; THALLAJ, N. 15, 11, 4935-4939. Research Journal of Pharmacy and Technology, 2022.
- 129) THALLAJ, N. Synthesis, characterization and analytical study of new imine compounds. Tishreen university journal, 2022, 44.2: 87-105.
- 130) THALLAJ, Nasser K.; MANDON, Dominique; WHITE, Kristen A. The Design of Metal Chelates with a Biologically Related Redox-Active Part: Conjugation of Riboflavin to Bis (2-pyridylmethyl) amine Ligand and Preparation of a Ferric Complex. 2007.
- 131) LABBAN, Louay. International Journ. IJMS, 2020, 5.12: 23-36.
- 132) LABBAN, Louay, et al. Pain-Relieving Properties of Ginger (Z. officinale) and Echinacea (E. angustifolia) Extracts Supplementation among Female Patients with Osteoarthritis. A Randomized Study. A Randomized Study. Advances in Medical, Dental and Health Sciences, 2020, 3.3: 45-48.
- 133) BESHER, Shaza, et al. Influence of soil salinity on the chemical composition of essential oil of Rosmarinus officinalis in Syria. Research Journal of Pharmacy and Technology, 2024, 17.5: 2282-2288.
- 134) THALLAJ, Nasser. Efficiency in transporting molecular oxygen to iron (II) complexes with ligands type tri (2-pyridylmethyl) amine substitution aromatic in (α) position by a mechanism that mimics biological oxidation. Journal homepage: www. ijrpr. com ISSN, 2021, 2582: 7421.
- 135) THALLAJ, Dr NK. Ferrous Complexes with Bis (Meo) in A-Substituted Tris (Pyridin-2-Ylmethyl) Amine Ligands: Effect of the Bis (Meo) in A-Substituents in Dioxygen Activation and Biomimetic Reactivity. Indian journal of advanced chemistry, 2021, 1.2: 20-26.
- 136) MACHKOUR, A., et al. Chemistry. 2006 Aug 25; 12 (25): 6660-8. P. DOI: https://doi.org/10.1002/chem, 200600276.
- 137) KHATIB, Osama, et al. The Global Impact of HIV: A Comprehensive Review. International Journal of Advanced Pharmaceutical Sciences and Research (IJAPSR), 2024, 4.3: 6-19.
- 138) THALLAJ, Nasser K., et al. Steric congestion at, and proximity to, a ferrous center leads to hydration of α-nitrile substituents forming coordinated carboxamides. Inorganic chemistry, 2014, 53.15: 7824-7836.
- 139) ABBOOD, Ayat, et al. In vitro Study for Antibiotic resistance of bacteria causing Urinary Tract Infection from Syrian adults. Research Journal of Pharmacy and Technology, 2022, 15.10: 4727-4732.
- 140) Thallaj NK, Orain PY, Thibon A, Sandroni M, Welter R, Mandon D. Inorg Chem. 2014 Aug 4; 53 (15): 7824-36. P7826-7828. DOI: https://doi. org/10.1021/ic500096h.
- 141) THALLAJ, N. K., et al. Inorg Chem. 2014 Aug 4; 53 (15): 7824-36. P7826-7828. DOI: https://doi.org/10.1021/ic500096h.
- 142) WANE, A.; THALLAJ, N. K.; MANDON, D. Chemistry. 2009 Oct 12; 15 (40): 10593-602. P10594-10595-10595.

ISSN: 1673-064X

E-Publication: Online Open Access

Vol: 68 Issue 10 | 2025

DOI: 10.5281/zenodo.17321958

- 143) LABBAN, Louay; THALLAJ, Nasser; AL MASRI, Mohammad. The Nutritional Value of Traditional Syrian Sweets and Their Calorie Density. World, 2019, 3.4: 40-47.
- 144) THALLAJ, Nasser. Quick Review of Chemistry Related to the [Fe]-Hydrogenases. International Journal of Advanced Pharmaceutical Sciences and Research (IJAPSR), 2022, 2.4: 1-15.
- 145) ABBOOD, Ayat; MALEK, Zeina; THALLAJ, Nasser. Antibiotic resistance of urinary tract pathogens in Syrian children. Research Journal of Pharmacy and Technology, 2022, 15.11: 4935-4939.
- 146) THALLAJ, Nasser. A short review of some examples of the binding of fullerenes C60 to transition metal complexes. International Journal of Advanced Pharmaceutical Sciences and Research (IJAPSR), 2022, 2.6: 1-12.
- 147) THALLAJ, N. Synthesis of a New Ligand Tris (2-pyridylmethyl) amine functionalized by a methoxy group and study of Dichloroferrous complexes, its reactivity to dioxygen both in the presence and absence of substrate. International Journal of Applied Chemical and Biological Sciences, 2021, 2.4: 65-77.
- 148) THALLAJ, Nasser. Review of a few selected examples of intermolecular dioxygenases involving molecular oxygen and non-heme iron proteins. Int. J. Adv. Parmacutical Sci. Res. (IJAPSR), 2023, 3: 1-18.
- 149) THALLAJ, Nasser. Microwave-Assisted Synthesis of Oxadiazole and Thiazolidine Derivatives. Indian journal of advanced chemistry, 2022, 1.3: 2022.
- 150) MACHKOUR, Ahmed, et al. The Coordination Chemistry of FeCl3 and FeCl2 to Bis [2-(2, 3-dihydroxyphenyl) -6-pyridylmethyl] (2-pyridylmethyl) amine: Access to a Diiron (iii) Compound with an Unusual Pentagonal-Bipyramidal/Square-Pyramidal Environment. Chemistry—A European Journal, 2006, 12.25: 6660-6668.
- 151) LABBAN, Louay; THALLAJ, Nasser. The effect of magnesium supplementation on Hba1c level and lipid profile among type 2 diabetics. Acta Scientific Nutritional Health, 2019, 3.10: 7-12.
- 152) LABBAN, Louay; THALLAJ, Nasser; MALEK, Zeina. The implications of E-cigarettes or" vaping" on the nutritional status. Jour Med Resh and Health Sci, 2019, 2.11: 784-787.
- 153) THALLAJ, Nasser K., et al. Square pyramidal geometry around the metal and tridentate coordination mode of the tripod in the [6-(3'-cyanophenyl)-2-pyridylmethyl] bis (2-pyridylmethyl) amine FeCl 2 complex: a solid-state effect. New Journal of Chemistry, 2005, 29.12: 1555-1558.
- 154) LABBAN, Louay; THALLAJ, Nasser. The medicinal and pharmacological properties of Damascene Rose (Rosa damascena): A review. Int. J. Herb. Med, 2020, 8.2: 33-37.
- 155) THALLAJ, Nasser K., et al. Reactivity of Molecular Dioxygen towards a Series of Isostructural Dichloroiron (III) Complexes with Tripodal Tetraamine Ligands: General Access to μ-Oxodiiron (III) Complexes and Effect of α-Fluorination on the Reaction Kinetics. Chemistry–A European Journal, 2008, 14.22: 6742-6753.
- 156) THALLAJ, Nasser K., et al. A ferrous center as reaction site for hydration of a nitrile group into a carboxamide in mild conditions. Journal of the American Chemical Society, 2008, 130.8: 2414-2415.
- 157) LABBAN, Louay; THALLAJ, Nasser; LABBAN, Abear. Assessing the level of awareness and knowledge of COVID 19 pandemic among syrians. Arch Med, 2020, 12.2: 8.